JCI The Journal of Clinical Investigation

Metabolic reprogramming of alloantigen-activated T cells after hematopoietic cell transplantation

Hung D. Nguyen, … , Shikhar Mehrotra, Xue-Zhong Yu

J Clin Invest. 2016;126(4):1337-1352. https://doi.org/10.1172/JCI82587.

Research Article **Immunology**

Alloreactive donor T cells are the driving force in the induction of graft-versus-host disease (GVHD), yet little is known about T cell metabolism in response to alloantigens after hematopoietic cell transplantation (HCT). Here, we have demonstrated that donor T cells undergo metabolic reprograming after allogeneic HCT. Specifically, we employed a murine allogeneic BM transplant model and determined that T cells switch from fatty acid β-oxidation (FAO) and pyruvate oxidation via the tricarboxylic (TCA) cycle to aerobic glycolysis, thereby increasing dependence upon glutaminolysis and the pentose phosphate pathway. Glycolysis was required for optimal function of alloantigen-activated T cells and induction of GVHD, as inhibition of glycolysis by targeting mTORC1 or 6-phosphofructo-2-kinase/fructose-2,6-biphosphatase 3 (PFKFB3) ameliorated GVHD mortality and morbidity. Together, our results indicate that donor T cells use glycolysis as the predominant metabolic process after allogeneic HCT and suggest that glycolysis has potential as a therapeutic target for the control of GVHD.

Metabolic reprogramming of alloantigen-activated T cells after hematopoietic cell transplantation

Hung D. Nguyen,[1] Shilpak Chatterjee,[1] Kelley M.K. Haarberg,[2] Yongxia Wu,[1] David Bastian,[1] Jessica Heinrichs,[1,3] Jianing Fu,[1,4] Anusara Daenthanasanmak,[1] Steven Schutt,[1] Sharad Shrestha,[5] Chen Liu,[6] Honglin Wang,[7] Hongbo Chi,[5] Shikhar Mehrotra,[1] and Xue-Zhong Yu[1,8]

[1]Department of Microbiology and Immunology, Medical University of South Carolina, Charleston, South Carolina, USA. [2]Transplant Immunology Laboratory, Northwestern University, Feinberg School of Medicine Comprehensive Transplant Center, Chicago, Illinois, USA. [3]Department of Immunology, H. Lee Moffitt Cancer Center, Tampa, Florida, USA. [4]Columbia Center for Translational Immunology, Columbia University, New York City, New York, USA. [5]Department of Immunology, St. Jude Children's Research Hospital, Memphis, Tennessee, USA. [6]Rutgers-Robert Wood Johnson Medical School, New Brunswick, New Jersey, USA. [7]Shanghai Institute of Immunology, Shanghai Jiao Tong University School of Medicine, Shanghai, China. [8]Department of Medicine, Medical University of South Carolina, Charleston, South Carolina, USA.

Alloreactive donor T cells are the driving force in the induction of graft-versus-host disease (GVHD), yet little is known about T cell metabolism in response to alloantigens after hematopoietic cell transplantation (HCT). Here, we have demonstrated that donor T cells undergo metabolic reprograming after allogeneic HCT. Specifically, we employed a murine allogeneic BM transplant model and determined that T cells switch from fatty acid β-oxidation (FAO) and pyruvate oxidation via the tricarboxylic (TCA) cycle to aerobic glycolysis, thereby increasing dependence upon glutaminolysis and the pentose phosphate pathway. Glycolysis was required for optimal function of alloantigen-activated T cells and induction of GVHD, as inhibition of glycolysis by targeting mTORC1 or 6-phosphofructo-2-kinase/fructose-2,6-biphosphatase 3 (PFKFB3) ameliorated GVHD mortality and morbidity. Together, our results indicate that donor T cells use glycolysis as the predominant metabolic process after allogeneic HCT and suggest that glycolysis has potential as a therapeutic target for the control of GVHD.

Introduction

Graft-versus-host disease (GVHD), caused by alloreactive donor T cells, is a major factor limiting successful allogeneic hematopoietic cell transplantation (allo-HCT) (1). Cell metabolism determines T cell fate and function. The metabolic profile of T cells varies in different immunological disorders such as arthritis, rheumatoid arthritis (RA), and systemic lupus erythematosus (SLE), and colitis (2–5). Furthermore, targeting T cell metabolism has been validated as a promising approach for treating these immunological diseases in preclinical models (5–7). However, the metabolic profile of T cells activated by alloantigens in vivo is still unclear, and understanding how T cells reprogram their metabolic pathways in response to alloantigens in vivo would provide rationale to target alloreactive T cell metabolism for the prevention of GVHD or graft rejection.

Generally, cells metabolize glucose to pyruvate via glycolysis and oxidize this pyruvate in the tricarboxylic (TCA) cycle for energy (8). Conversely, a large body of work indicates that lymphocytes activated in vitro do not follow this trend, but rather convert this pyruvate to lactate (9, 10). In vitro–activated T cells increase glycolysis and glutamine consumption in conjunction with a downregulation of fatty acid (FA) and TCA oxidative function (9). Studies from Ferrara's group have indicated that alloreactive T cells increase FA oxidation (FAO) and that targeting FAO could arrest GVHD (11, 12). However, this observation is contrary to the paradigm that glucose uptake and glycolysis are required for activated T cells to meet their increased demand for energy (8) and subsequently induce GVHD (10). Together, the metabolic profile of alloantigen-activated T cells in vivo may be different from that of activated T cells in vitro.

mTOR acts as a metabolic sensor of nutrients (13) and functions as a central regulator of cell metabolism, growth, proliferation, and survival (14). mTOR is composed of mTOR complex 1 (mTORC1) and mTORC2. Traditionally, mTORC1 is crucial for differentiation of T cells into Th1 and Th17 subsets, whereas mTORC2 is required for differentiation into the Th2 subset (14, 15). However, new evidence indicates that mTORC1 plays a predominant role in regulating T cell priming and in vivo immune responses, while RICTOR-mTORC2 and RHEB exert modest effects (16). mTORC1 also regulates the generation and function of induced Tregs (iTregs) (17). In vitro inhibition of mTORC1 by rapamycin reduces glycolytic activity and mitochondrial mass of T cells (18). While rapamycin has previously been employed as a treatment for GVHD, its efficacy, specificity (19–21), and toxicity (21, 22) obscure whether mTOR is a valid target for the control of GVHD. Moreover, the effect of mTOR on T cell metabolism after HCT and the differential contributions of mTORC1 and mTORC2 in GVHD development remains unclear.

In the current study, we demonstrate that T cells undergo distinct metabolic reprogramming in response to alloantigens in vivo and propose that alloreactive T cells preferentially depend on glycolysis to meet bioenergetic demands. Furthermore, we propose that targeting glycolysis may represent a promising strategy to control GVHD.

Conflict of interest: The authors have declared that no conflict of interest exists.
Submitted: April 30, 2015; **Accepted:** January 21, 2016.
Reference information: *J Clin Invest*. 2016;126(4):1337–1352. doi:10.1172/JCI82587.

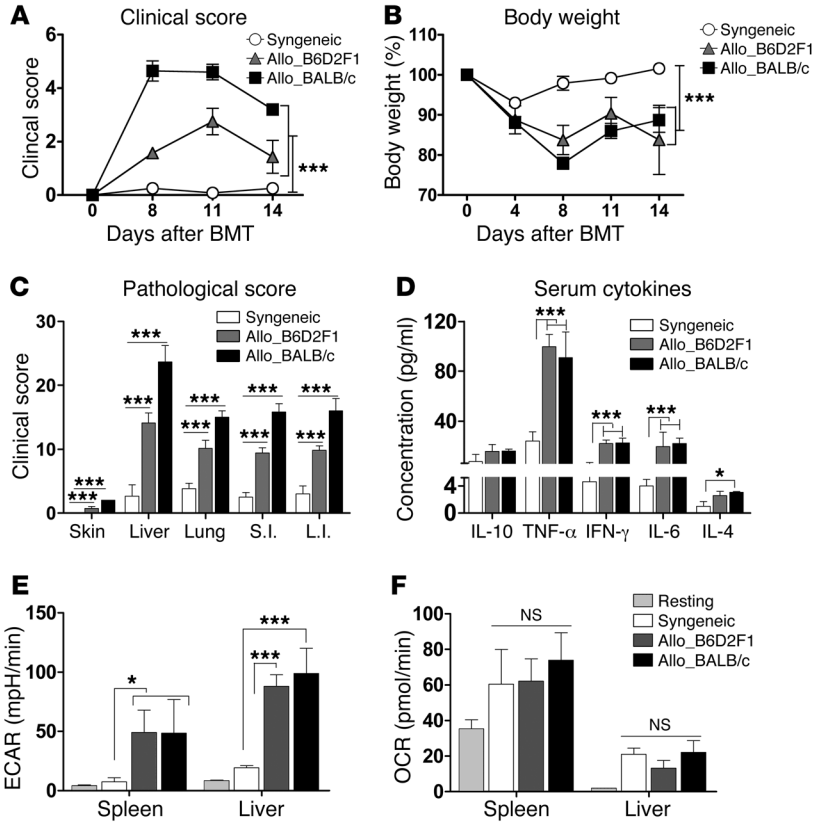

Figure 1. Donor T cells preferentially increase glycolysis in response to alloantigens in vivo. Lethally irradiated B6, B6D2F1 (1,100 cGy), or BALB/c (700 cGy) mice were transplanted with 5×10^6/mouse TCD-BM plus 1–2 × 10^6/mouse T cells isolated from B6 donors. After 14 days, recipients were euthanized, and blood and organs were collected. (**A** and **B**) The GVHD clinical score (**A**) and body weight loss (**B**) during experimental time course are shown. (**C**) Pathological score are indicated in recipient skin, liver, lung, small intestine (S.I.), and large intestine (L.I.). (**D**) Cytokine levels in the recipient sera are displayed. T cells were isolated from spleens or livers of the syngeneic or allogeneic recipients and measured for ECAR and OCR. (**E** and **F**) Summary of ECAR (**E**) or OCR (**F**) rate of T cells from recipient spleen or liver on day 14 after BMT. (**A**–**D**) Data were representative of three experiments (n = 7–10 per group). (**E** and **F**) The data were combined from three independent experiments (n = 15 per group). Bar graph shows the mean ± SEM. $^*P < 0.05$; $^{***}P < 0.001$, Mann-Whitney U test (**A** and **B**), two-tailed Student t test (**C**–**F**).

Results

T cells undergo metabolic reprogramming in response to alloantigens in vivo after BM transplantation. To understand how allogeneic T cells reprogram their metabolic pathways to fulfill bioenergetic and biosynthetic demands adapted upon activation in vivo, we utilized two murine models of allogeneic BM transplantation (BMT), B6 (H-2^b) → BALB/c (H-2^d) and B6 (H-2^b) → B6D2F1 (H-$2^{b/d}$), to recapitulate the process of T cell response to alloantigen in vivo. Switching from oxidative phosphorylation (OXPHOS) to glycolysis is the hallmark of in vitro–activated T cell metabolism (9, 23, 24). Hence, we first determined the rates of glycolysis and OXPHOS in donor T cells after BMT by measuring extracellular acidification rate (ECAR; reflecting the rate of glycolysis indicated by lactate secretion) and oxygen consumption rate (OCR; reflecting OXPHOS). Allogeneic recipients developed more severe GVHD, illustrated by higher clinical score (Figure 1A), body weight loss (Figure 1B), and pathological damage in GVHD target organs (Figure 1C) compared with syngeneic recipients. Consistently, the levels of proinflammatory cytokines (TNF-α, IFN-γ, and IL-6) were significantly elevated in sera of allogeneic recipients when compared with those of the syngeneic recipients (Figure 1D). On day 14 after BMT, glycolysis and OXPHOS were significantly increased in the T cells isolated from spleens and livers of allogeneic or syngeneic recipients compared with those freshly isolated naive donor T cells (Figure 1, E and F). While the OCR values of donor T cells isolated from syngeneic and allogeneic recipients were comparable (Figure 1F), the glycolytic activity of donor T cells was significantly greater in allogeneic than syngeneic recipients in the spleens and livers (Figure 1E), indicating an escalation of glucose metabolism correlated with GVHD development. Furthermore, T cells isolated from the livers of allogeneic recipients exhibited even higher ECAR values compared with those from the spleens on day 14 after BMT, implying higher glycolytic activity of alloreactive T cells in GVHD target organs (Figure 1E).

To further understand the metabolic profile of donor T cells in response to alloantigens, using a mass spectrum–based metabolomic approach to quantify relative concentrations of metabolites, we compared the metabolic changes in donor T cells transplanted into syngeneic B6 versus allogeneic BALB/c recipients at day 4 (early preclinical stage), day 7 (preclinical stage), and day 14 (clinical stage) after BMT. Compared with the freshly isolated resting T cells, donor T cells retrieved from allogeneic or syngeneic recipients accumulated substantial amounts of metabolites involved in anabolic pathways of lipids, amino acids, nucleotides, and carbohydrates as displayed in the heat map (Figure 2A). Consistent with the escalating glycolytic activity observed in the bioenergetic analysis (Figure 1E), the mRNA level of lactate dehydrogenase (*Ldh*), which catalyzes the conversion of pyruvate to lactic acid, and *Mtc4*, mediating lactic acid efflux, were both significantly higher in allogeneic T cells versus their syngeneic counterparts (Figure 2C). Glucose, NAD^+, and phosphate, which are required for glycolysis, were significantly decreased in allogeneic T cells compared with resting T cells, reflecting an increased demand for these components to support the glycolytic pathway (Figure 2B). Consistently, donor T cells in allogeneic recipients exhibited significantly higher levels of the glycolytic intermediate glucose 6-phosphate (G-6P) than in syngeneic recipients at all three time points measured after BMT (Figure 2B). Expression of the mRNAs encoding for hexokinase

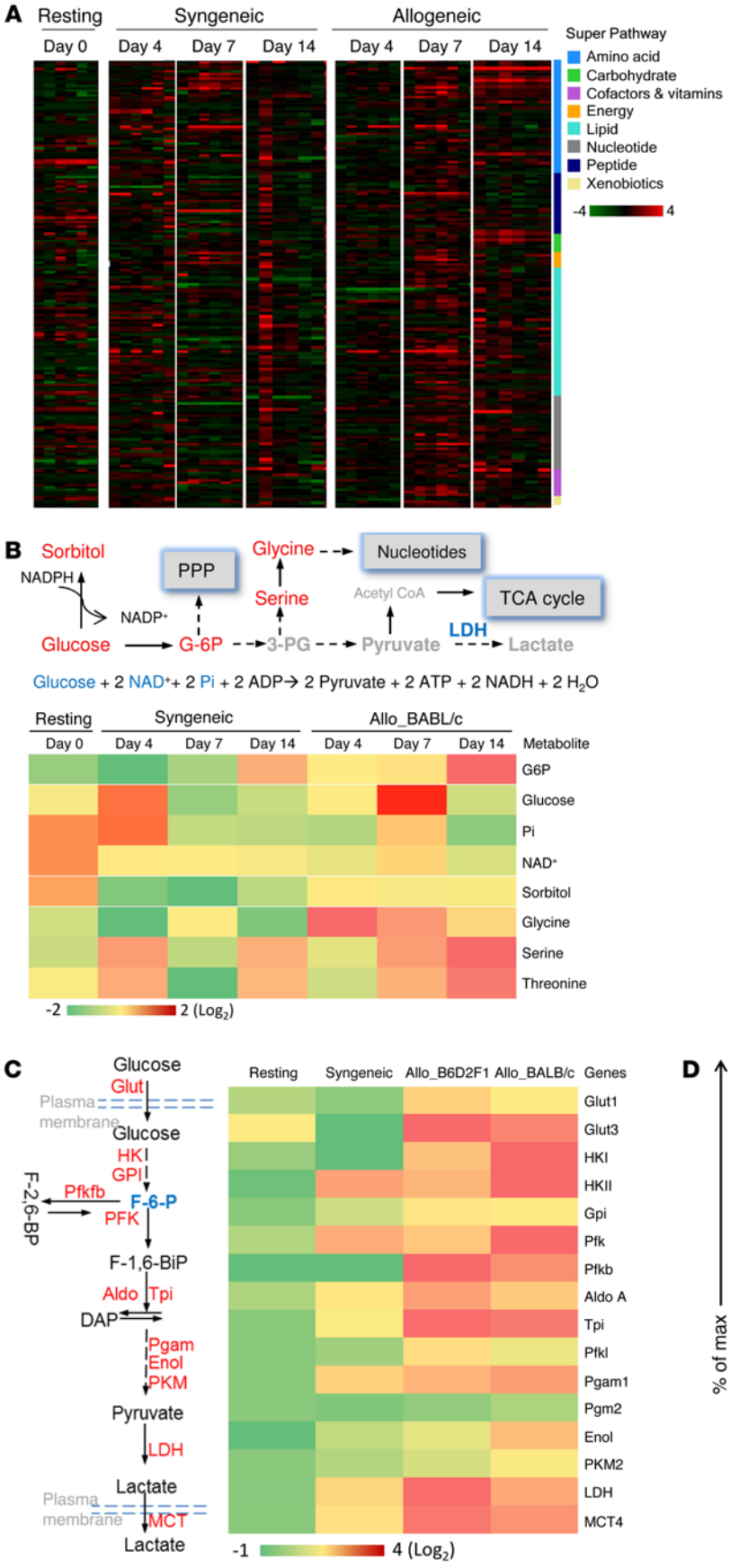

Figure 2. T cells undergo metabolic reprogramming in response to alloantigens after BMT. T cells were isolated from allogeneic BALB/c and syngeneic B6 recipient spleens at indicated times after BMT and measured for intracellular metabolites by mass spectrometry. (**A**) The heat map represents the $\log_2$ value of the relative amount of each metabolite, which is grouped in the indicated metabolic pathway. (**B**) The glycolytic pathway is elucidated and the key metabolites measured are highlighted in red. (**C**) The mRNA expression of the metabolic genes of glycolytic pathway was determined by qPCR on the donor T cells from allogeneic or syngeneic recipients at 14 days after BMT. The relative level of mRNA is based on the resting T cells as 1. (**D**) The glucose uptake activity and GLUT1 expression in donor T cells from allogeneic or syngeneic recipients were determined by flow cytometry. Data are shown as mean ± SD (**A** and **B**, $n = 6$; **C**, $n = 3$; **D**, $n = 7$–10). $^*P < 0.05$, $^{***}P < 0.001$, 2-tailed Student t test (**D**). The metabolite expression profile and the input gene list are provided in Supplemental Tables 1–3 and Supplemental Table 4, respectively.

isoform 1 (HK1) and HK2, which catalyze the conversion of glucose to G-6P, were also higher in T cells from allogeneic recipients than those from syngeneic recipients or resting T cells (Figure 2C). Because HK1 and HK2 can quickly fluctuate (25), both can contribute to rapid induction of glycolysis in alloantigen-activated T cells. Contrary to in vitro–activated T cells that primarily increase *HK2* gene expression (9), T cells activated by alloantigen in vivo increased *HK1* (Figure 2C). The relative levels of glycine, serine, and threonine are significantly increased in T cells from allogeneic recipients 14 days after BMT, reflecting an elevated level of 3-phosphoglycerate (Figure 2B). Consistently, the enzymes *Aldo* and *Tpi*, which catalyze the conversion of fructose 1,6-bisphosphate (F1,6-BiP) to 3-phosphoglycerate, were significantly upregulated in the T cells from allogeneic compared with those from syngeneic recipients (Figure 2C). Donor T cells in allogeneic recipients also exhibited a significantly higher level of sorbitol, indicating an increase in glucose transport, which can be subsequently used for both glycolysis and pentose phosphate pathway (PPP) (Figure 2B). Additionally, allogeneic T cells significantly increased their glucose uptake capacity, reflected by elevated 2-NBDG expression, level of mRNAs encoding *Glut1* and *Glut3*, and surface expression of GLUT1 (Figure 2D). GLUT1 and GLUT3 are critical enzymes regulating glucose transport in activated T cells (10). Moreover, the levels of the mRNAs encoding metabolic enzymes involved in the most important steps of the glycolytic pathway were substantially elevated in allogeneic T cells compared with those in syngeneic or resting T cells (Figure 2C). Taken together, these results indicate that donor T cells upregulate the glycolytic pathway after BMT. Importantly, T cells further increase glycolysis in response to alloantigen, suggesting that an escalating rate of glycolysis is correlated with GVHD development.

Upon activation in vitro, T cells utilize various pathways to meet their increased metabolic demand for activation and proliferation (9, 12). Among them, TCA cycle-generated FAO was reported as a major fuel source to support T cell activation during GVHD induction (11). However, we observed that during an allogeneic response, carnitine, deoxycarnitine, and acylcarnitines required for FAO were diminished in the T cells from either allogeneic or syngeneic recipients after BMT, as compared with those resting donor T cells (Figure 3, A and B). Similarly, donor T cells from allogeneic and syngeneic recipients significantly downregulated mitochondria-dependent FAO and pyruvate oxidation through the TCA cycle after BMT, reflected by decreased levels of TCA cycle intermediates including citrate, fumarate, malate, and free coenzyme A (CoA) (Figure 3, A and B). Noticeably, the levels of these metabolites were dramatically lower in allogeneic T cells compared with both syngeneic and resting T cells, suggesting an independence of allogeneic T cells from FAO after BMT and confirming that the decrease in components required for FAO (carnitine, deoxycarnitine, and acylcarnitines) was not due to cellular demand. Correlating with the metabolomic data, the FA uptake reflected by BoDipy labeling was significantly lower in the T cells from allogeneic than those from syngeneic recipients 14 days after BMT (Figure 3C and Supplemental Figure 3, A and B; supplemental material available online with this article; doi:10.1172/JCI82587DS1). Protein level of CPT1A and mRNA levels of *Pgc1a* were comparable in the T cells from allogeneic or syngeneic recipients (Figure 3, D–F, and Supplemental Figure 3, D–F), even though mRNA level of *Cpt1a* in allogeneic T cells was dependent on allo-BMT models (Figure 3F and Supplemental Figure 3C). The lower levels of TCA cycle metabolites could also be due to the fact that glucose-generated pyruvate in alloactivated T cells was converted to lactate instead of metabolized in the TCA cycle. Together, the decrease in FAO through TCA observed from in vivo–activated T cells was similar to that observed from in vitro–activated T cells. However, T cells activated by alloantigens in vivo significantly diminished TCA cycle metabolite levels, whereas in vitro–activated T cells remained unchanged (9).

In contrast to a decrease in FA uptake, we observed that donor T cells accumulated long-chain FAs on days 7 and 14 in allogeneic recipients (Figure 3A). This is likely an indication of a decline in oxidation or an increase in complex lipid hydrolysis and lipid synthesis. Hydrolysis of the lipid membrane was reflected by elevated levels of lysolipid species that contain ethanolamine, inositol, or phosphocholine as head groups, which are derived from phospholipids enriched in the inner leaflet of the cell membrane (Figure 3A). An increase in FA synthesis was supported by elevated levels of the mRNAs encoding enzymes involved in FA synthesis pathway (data not shown). Therefore, these data suggest that, in order to obtain lipid materials needed for proliferation, alloantigen-activated T cells not only reduce FAO in TCA but also increase intrinsic lipolysis and FA synthesis.

Upon activation, energy production in T cells activated in vitro is known to couple glycolysis with glutamine catabolism (9). This coupling is not only tightly linked to different biosynthetic pathways but also generates the anaplerotic substrate α-ketoglutarate (α-KG), which can be metabolized through the TCA cycle to generate either citrate or pyruvate, a process known as glutaminolysis (Supplemental Figure 1A). In the current study, we observed an increased expression of mRNAs encoding enzymes that regulate glutamine metabolism in allogeneic T cells compared with syngeneic or resting T cells (Supplemental Figure 1C). These enzymes included SCL2a5, SCL3a2, and SCL7a, which control glutamine transport; glutamine-fructose-6-phosphate transaminase (Gfpt1), phosphoribosyl pyrophosphate amidotransferase (PPAT), and glutaminase 2 (GLS2), which control the conversion of glutamine to glutamate; and glutamate dehydrogenase 1 (GLUD1), glutamate oxaloacetate transaminase (GOT), and ornithine aminotransferase (OAT), which control the conversion of glutamate to α-KG. Consistent with the increase in mRNA expression of *Scl2a5*, *Scl3a2*, *Scl7a*, the relative level of glutamine was significantly higher in T cells from transplanted recipients compared with resting T cells (Supplemental Figure 1, B and C, Supplemental Table 7). Simultaneously, the level of glutamate was lower and the levels of aspartate (Asp) and ornithine (Orn) — the products of converting glutamate to α-KG by OAT and GOT, respectively – were higher in the T cells from allogeneic than those from syngeneic recipients on day 14 after BMT, suggesting that allogeneic T cells further increase glutaminolysis by producing the anaplerotic substrate α-KG, which is likely used for replenishing the intermediate metabolites of the TCA cycle. Intriguingly, the metabolic enzyme OAT also links glutamine to Orn synthesis and subsequently converts Orn to polyamines, such as putrescine in urea cycle (Supplemental Figure 1A). Along these lines, the levels of putrescine and Orn decar-

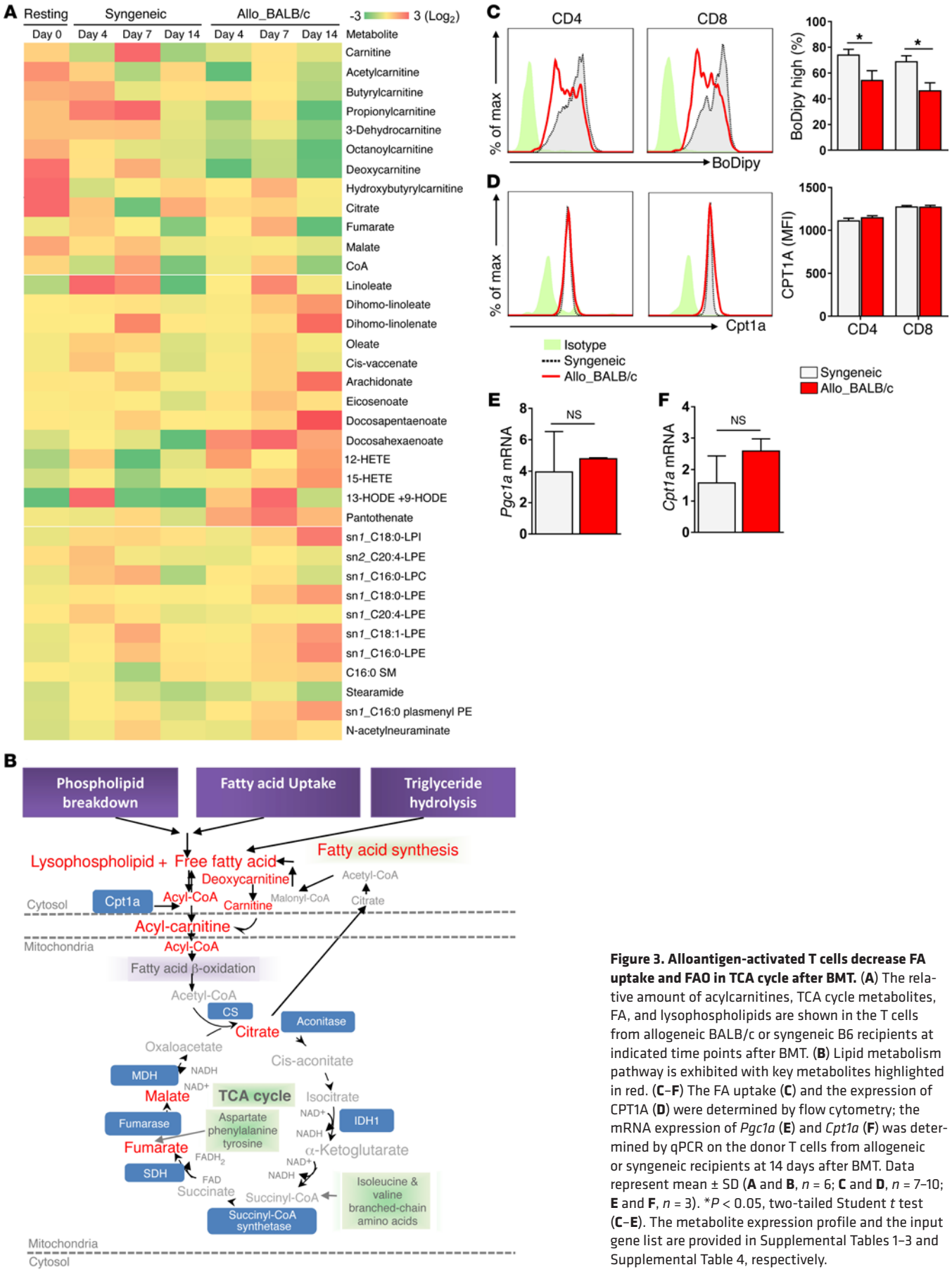

Figure 3. Alloantigen-activated T cells decrease FA uptake and FAO in TCA cycle after BMT. (**A**) The relative amount of acylcarnitines, TCA cycle metabolites, FA, and lysophospholipids are shown in the T cells from allogeneic BALB/c or syngeneic B6 recipients at indicated time points after BMT. (**B**) Lipid metabolism pathway is exhibited with key metabolites highlighted in red. (**C**–**F**) The FA uptake (**C**) and the expression of CPT1A (**D**) were determined by flow cytometry; the mRNA expression of *Pgc1a* (**E**) and *Cpt1a* (**F**) was determined by qPCR on the donor T cells from allogeneic or syngeneic recipients at 14 days after BMT. Data represent mean ± SD (**A** and **B**, $n = 6$; **C** and **D**, $n = 7$–10; **E** and **F**, $n = 3$). *$P < 0.05$, two-tailed Student t test (**C**–**E**). The metabolite expression profile and the input gene list are provided in Supplemental Tables 1–3 and Supplemental Table 4, respectively.

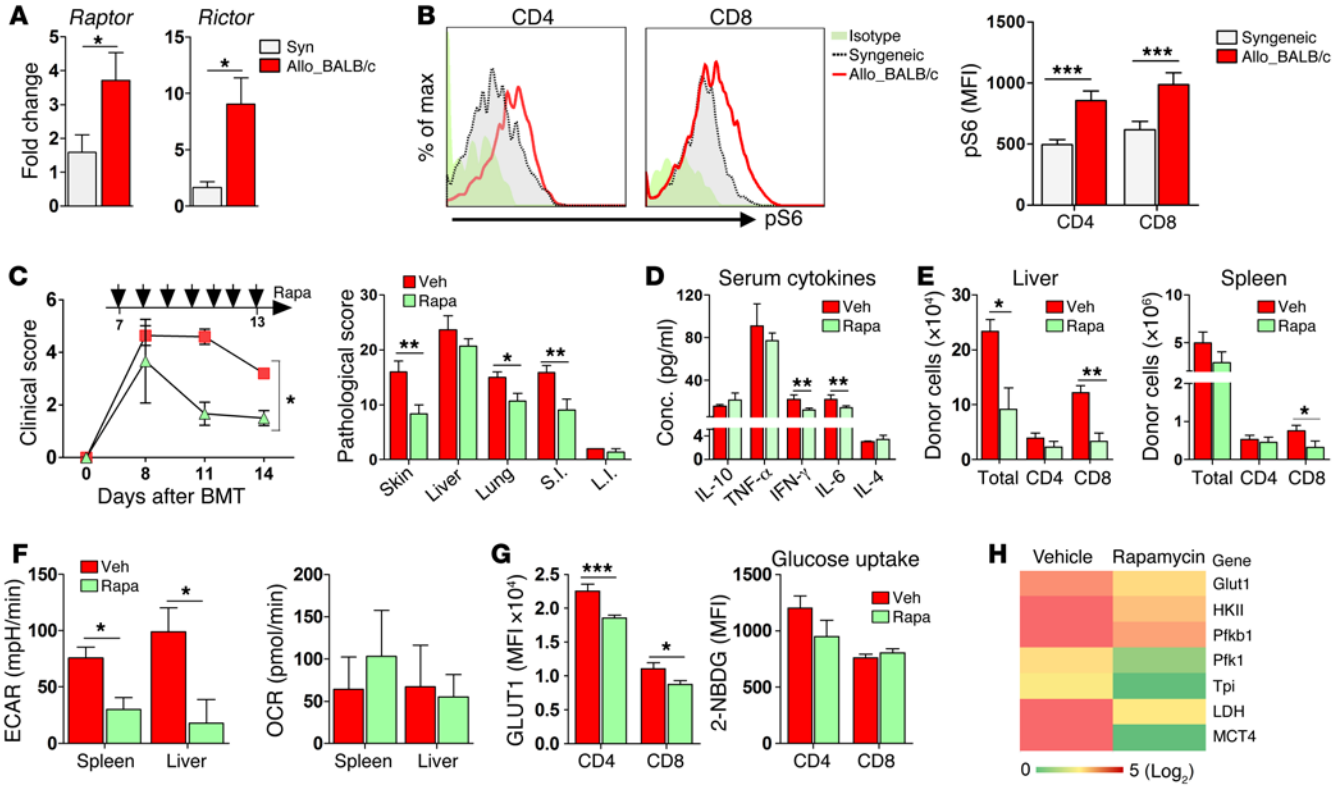

Figure 4. Delayed rapamycin treatment reduces GVHD through decreasing glycolytic activity in donor T cells. (**A** and **B**) Relative levels of *Raptor* and *Rictor* mRNA (**A**), and pS6 expression (**B**) are shown in T cells from allogeneic BALB/c and syngeneic B6 recipients at 14 days after BMT (**C**–**H**) Lethally irradiated BALB/c mice were transplanted with 5×10^6/mouse TCD-BM from B6 Ly5.1 mice plus 1×10^6/mouse T cells isolated from B6 donors. Recipients were administrated daily i.p. with rapamycin (1.5 mg/kg) or 0.5% methylcellulose (vehicle) started from day 7 until day 14 after BMT. (**C**) The GVHD clinical score monitored through experiment and the pathological score of GVHD target organs at the day 14 after BMT are shown. (**D**) The levels of serum cytokines are displayed. (**E**) Absolute numbers of donor H-2K^{b+}Ly5.1$^-$CD4$^+$ or CD8$^+$ T cells in recipient liver and spleen are depicted. (**F**) The bar graphs show ECAR and OCR values of spleens T cells or liver monocytes. (**G**) The expression of GLUT1 and glucose uptake are shown on the spleen T cells (Supplemental Figure 4A). Data are representative of two independent experiments with 5–7 mice per group. Error bars show mean ± SEM. $^*P < 0.05$; $^{**}P < 0.01$; $^{***}P < 0.001$, two-tailed Student *t* test (**A**, **B**, right panel of **C**, and **D**–**G**), and Mann-Whitney *U* test (**C**, left panel). (**H**) The heat map represents the $\log_2$ value of the relative individual mRNA expression of glycolytic enzymes in splenic T cells. The input gene list and expression profile are provided in Supplemental Table 5. Data are representative of two independent experiments ($n = 3$). S.I., small intestine; L.I., large intestine.

boxylase (ODC) that catalyze the decarboxylation of Orn to form putrescine were significantly higher in allogeneic T cells at all time points tested (Supplemental Figure 1, B and C). However, we cannot exclude that allogeneic T cells may also couple glutaminolysis with biosynthetic pathways to produce other metabolites such as γ butyric acid (GABA), which significantly accumulated at day 14 after BMT (Supplemental Figure 1, A and C).

Glycolysis interconnects with the PPP (Supplemental Figure 2A), and increases in glucose metabolism consequently impact PPP metabolism, which is necessary for nucleotide biogenesis, glutathione reduction, and NADPH regeneration (26). Indeed, the mRNA expression of metabolic regulating enzymes in the PPP was significantly higher in donor T cells from allogeneic than from syngeneic recipients at day 14 (Supplemental Figure 2B). Consistent with the upregulation of *Pgd*, the key metabolite product of this enzyme, pentulose 5-phosphate, was significantly higher in donor T cells from allogeneic compared with syngeneic recipients or resting T cells, indicating an accumulation of biomass for anabolic growth of T cells under allogeneic response (Supplemental Figure 2D). Furthermore, pyrimidine catabolism was significantly decreased in the T cells from allogeneic compared with those from syngeneic recipients (Supplemental Figure 2, C and D, and Supplemental Table 8), suggesting that PPP was preferentially utilized for biomass synthesis during proliferation and expansion.

mTORC1, not mTORC2, is crucial for maintaining glycolytic activity of alloantigen-activated T cells, which is required for inducing GVHD after allogeneic BMT. mTOR is a well-known metabolic sensor (13) that functions as a master regulator of glucose metabolism in activated lymphocytes (14). Thus, we sought to determine if there was any difference in mTOR signaling between T cells from allogeneic versus syngeneic recipients. Indeed, the mRNA levels of *Raptor* and *Rictor*, the adaptor proteins of mTORC (Figure 4A), and the level of phosphorylated S6 (pS6), a marker mTOR activity (Figure 4B), were significantly increased in T cells transplanted into allogeneic recipients as compared with those in syngeneic recipients 14 days after BMT. This data indicates a relationship between mTOR activation and GVHD induction. We next investigated the causality between these two processes by blocking glycolysis using rapamycin, an mTOR inhibitor (16, 27), which has been shown to ameliorate GVHD (28). To dissect the contribution of glycolysis in

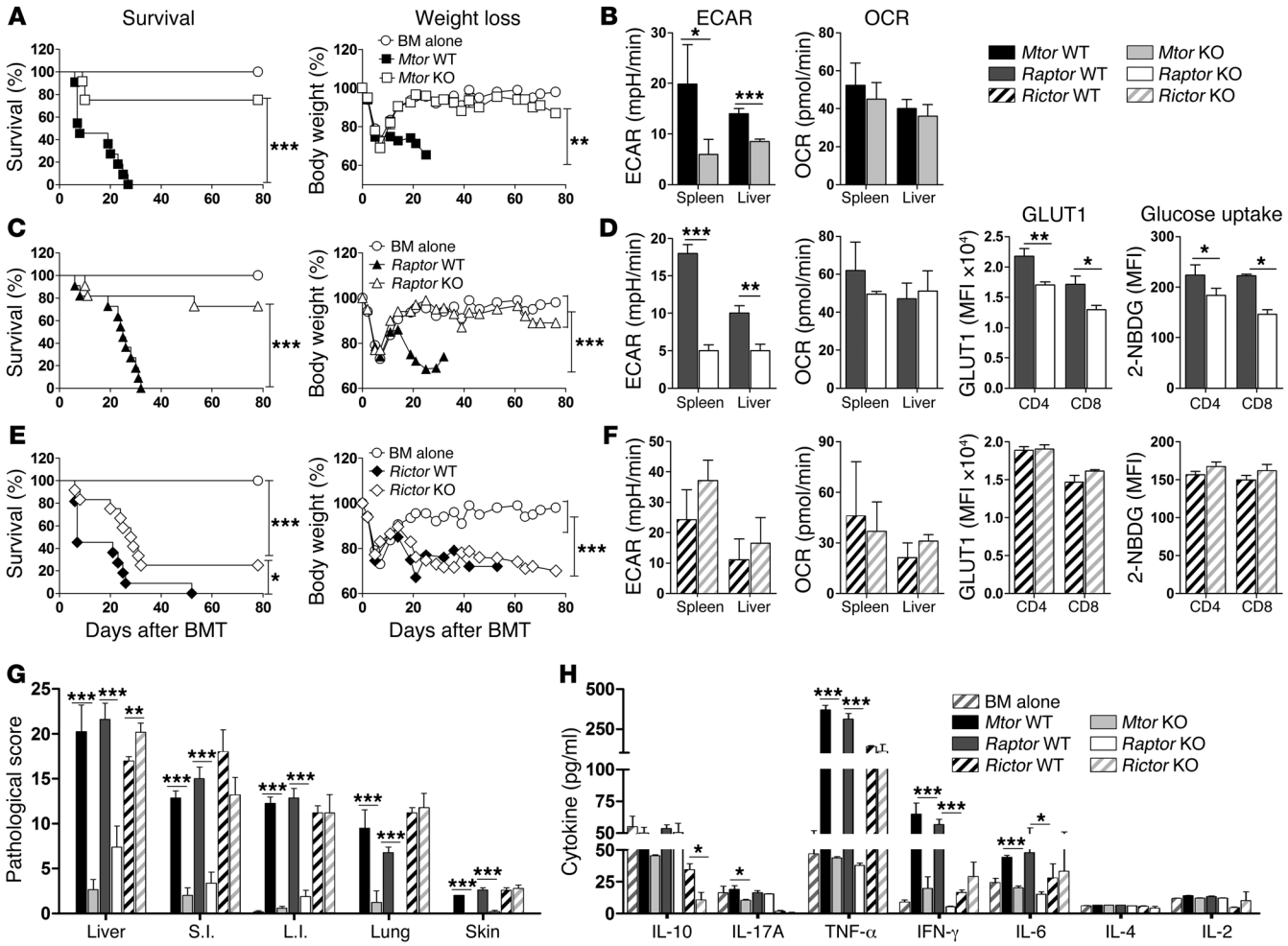

Figure 5. T cells deficient for mTOR or mTORC1 reduce glycolytic activity and fail to induce GVHD. Lethally irradiated BALB/c mice (n = 10–15 mice per group) were transplanted with TCD-BM alone or plus 1×10^6/mouse CD25–depleted T cells isolated from WT or KO donor mice on B6 background. (**A**, **C**, and **E**) Recipient survival and body weight loss are shown. In separate experiment, recipients (n = 5 mice per group) were euthanized at the day 14 after BMT. (**G**) Pathologic scores are indicated in recipient skin, liver, small intestine (S.I.), large intestine (L.I.), and lung 14 days after BMT. (**B**, **D**, and **F**) Summary of ECAR or OCR rate of T cells from recipient spleen and liver are shown. The glucose uptake activity and GLUT1 expression of T cells from recipient spleen were displayed (right panels). (**H**) Cytokine levels in recipient sera are shown. Data are representative of two independent experiments and at least 10 mice per group. Data are shown as mean ± SEM. $^*P < 0.05$; $^{**}P < 0.01$; $^{***}P < 0.001$, log-rank test (left panels of **A**, **C**, and **E**), Mann-Whitney U test (right panels of **A**, **C**, and **E**), two-tailed Student t test (**B**, **D**, and **F**–**H**).

T cell activation, rapamycin treatment was started from day 7 after BMT until termination of the experiment (Figure 4C). We observed that GVHD clinical and pathological scores (Figure 4C) were significantly decreased in recipients treated with rapamycin as compared with those treated with vehicle. Furthermore, the levels of serum proinflammatory cytokines — e.g., IFN-γ and IL-6 (Figure 4D) — and the numbers of donor T cells in recipient livers (Figure 4E) were dramatically reduced in the recipients treated with rapamycin. As expected, rapamycin profoundly decreased glycolytic activity of T cells isolated from allogeneic recipient spleens and livers, whereas OXPHOS activity was not affected (Figure 4F). Additionally, the levels of the mRNA coding enzymes involved in glycolysis were decreased (Figure 4H) and GLUT1 expression (Figure 4G and Supplemental Figure 4A) on donor T cells was significantly lower in T cells from rapamycin-treated recipients. Altogether, the inhibition of mTOR decreased T cell glycolytic activity after allo-BMT, which likely contributed to GVHD amelioration.

To further define the role of mTOR in glycolysis maintenance in GVHD-causing alloreactive T cells, we compared the pathogenicity of *Mtor* WT and KO T cells during GVHD induction using a conditional gene-targeting approach. Due to higher percentages of naive Tregs (nTregs) in the periphery of *Mtor* KO than WT mice (14), $CD25^+$ cells were depleted from T cell grafts prior to BMT to exclude the effect of nTregs on GVHD outcome. After being transplanted into allogeneic BALB/c recipients, CD25-depleted T cells from *Mtor* KO donors induced significantly less GVHD than WT counterparts, highlighted by improved recipient survival and weight loss (Figure 5A). Since mTOR signaling is composed of mTORC1 and mTORC2, each playing distinct roles in T cell differentiation and function (15, 16, 29), we sought to determine whether either mTORC1 or mTORC2, or both, are responsible for T cell pathogenicity in GVHD. To address this question, we used donor mice that were selectively deficient for *Raptor* or *Rictor* in which mTORC1 or mTORC2 was impaired, respectively. After BMT, the

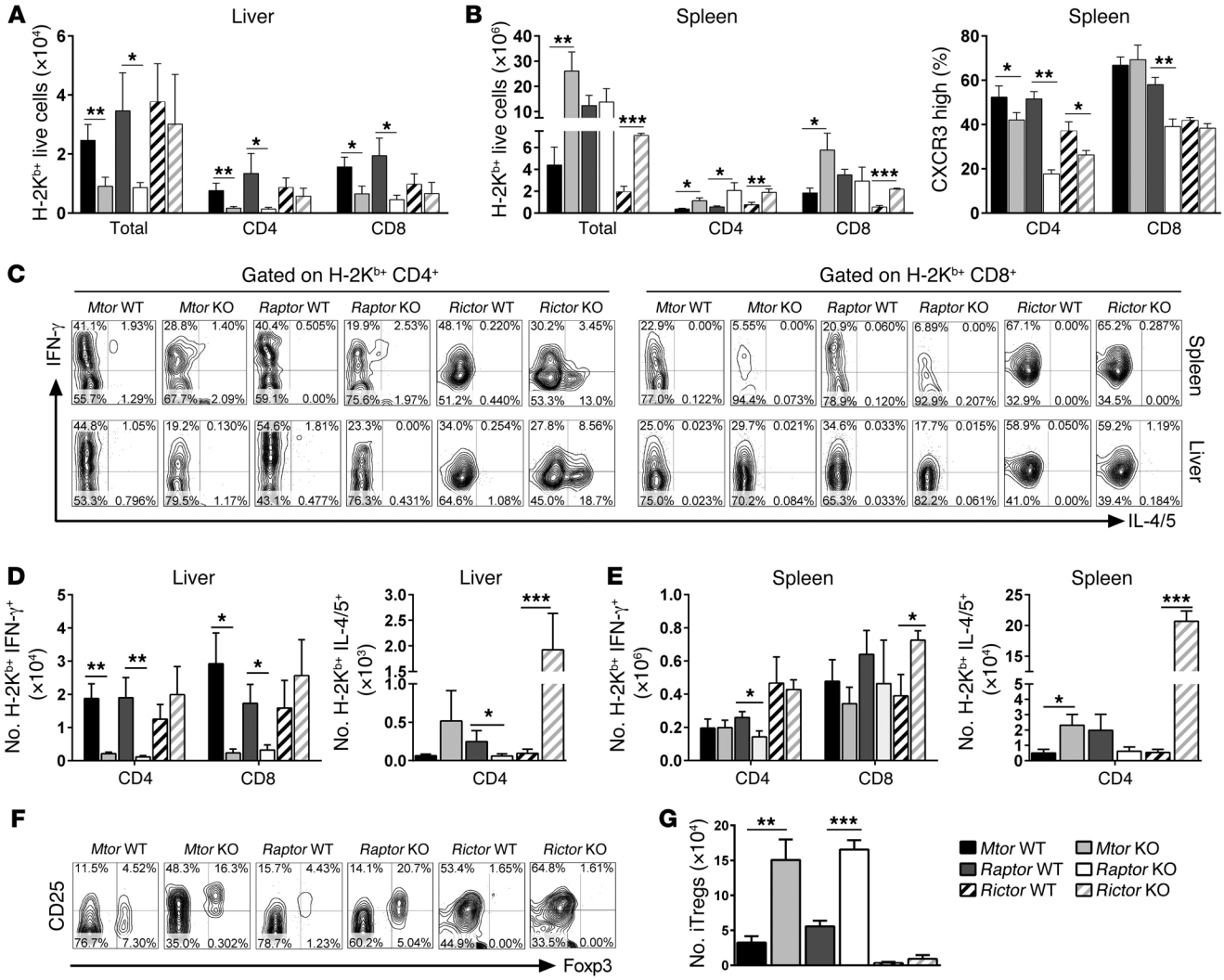

Figure 6. Ablation of mTOR or RAPTOR, not RICTOR, leads to a significant reduction in Th1 but enhancement in iTreg differentiation. Lethally irradiated BALB/c mice were transplanted with TCD-BM from B6 Ly5.1 donors alone or with CD25-depleted T cells at 1×10^6/mouse from WT or KO donors on B6 background. After 14 days, recipient mice were euthanized and blood, spleen, and livers were harvested. (**A** and **B**) Absolute numbers of donor H-2K^{b+}Ly5.1$^-$CD4$^+$ or H-2K^{b+}Ly5.1$^-$CD8$^+$ T cells in recipient liver (**A**) and spleen (**B**) are displayed. Summary of CXCR3 expression gated on H-2K^{b+}Ly5.1$^-$CD4$^+$ or CD8$^+$ T cells in the spleens are shown. (**C**) The percentages of IFN-γ– and IL-4/5–secreting cells from spleen or liver are shown in gated H-2K^{b+}Ly5.1$^-$CD4$^+$ or H-2K^{b+}Ly5.1$^-$CD8$^+$ T cells. (**D** and **E**) Total numbers of IFN-γ– or IL-4/5–secreting cells are shown on CD4$^+$ or CD8$^+$ donor T cells in recipient liver (**D**) or spleen (**E**). (**F**) The expression of CD25 and FOXP3 gated on donor CD4$^+$ spleen cells. (**G**)Absolute number of iTregs among donor T cells. Data are pooled from three independent experiments with 15 mice per group (mean ± SEM), $^*P < 0.05$; $^{**}P < 0.01$; $^{***}P < 0.001$, two-tailed Student *t* test (**A**, **B**, **D**, **E**, and **G**).

recipients of *Rictor* WT or KO T cells suffered from severe GVHD with a comparable weight loss and lethality (Figure 5E). In contrast, *Raptor* WT T cells caused severe weight loss and rapid lethality in all the recipients, whereas *Raptor* KO T cells only caused mild weight loss and lethality in a fraction of the recipients (Figure 5C). In support of these findings, pathologic evidence also showed the recipients of mTOR or *Raptor* KO, but not *Rictor* KO, T cells had significantly lower pathological scores than those of the respective WT T cells in each of the five target organs examined (Figure 5G). Consistently, the levels of TNF-α, IFN-γ, and IL-6 were also remarkably decreased in the sera of the recipients transplanted with *Mtor* or *Raptor* KO, but not *Rictor* KO T cells, when compared with those with WT T cells (Figure 5H). The levels of IL-2, IL-4, IL-10, and IL-17 were low or undetectable and not different among the seven groups of recipients (Figure 5H). Collectively, mTOR activation is required for T cells to induce GVHD, and mTORC1 — not mTORC2 — is responsible for T cell pathogenicity.

To understand how mTOR affects T cell metabolism in response to alloantigen in vivo, we examined the bioenergetic activity of donor T cells in recipients 14 days after BMT. *Raptor* or *Mtor* KO T cells, contrary to *Rictor* KO T cells, had significantly reduced glycolytic activity as compared with their counterparts in recipient spleens and livers (Figure 5, B, D, and F). Furthermore, glucose uptake and surface GLUT1 expression (Figure 5, D and F, and Supplemental Figure 4, B and C) were significantly decreased in *Raptor*, but not *Rictor*, KO T cells. In contrast, OXPHOS values for the KO T cells were not different from that of their respective WT counterparts (Figure 5, B, D, and F). These data indicate that

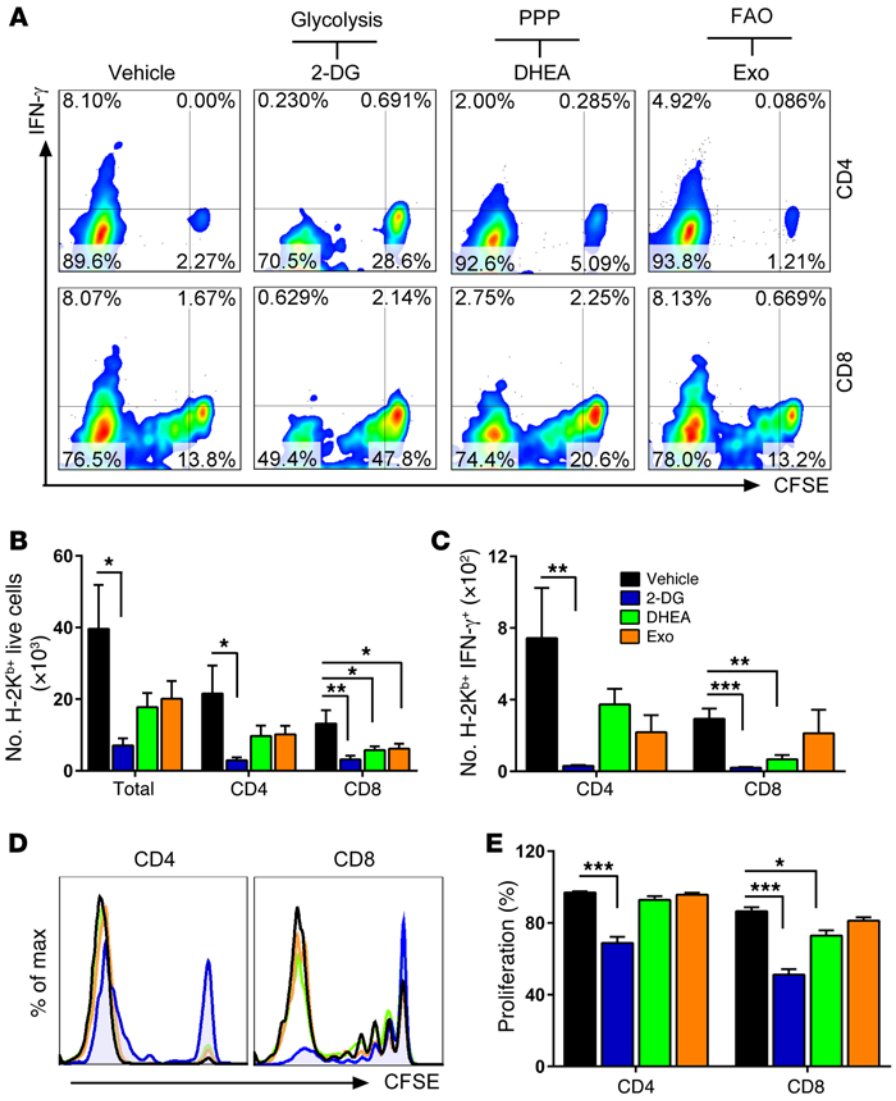

Figure 7. Glycolysis is required for T cell activation and proliferation in response to alloantigens after BMT. Lethally irradiated BALB/c mice were transplanted with 1.5 × 10^6 CFSE-labeled T cells from B6 donors and administrated i.p. with 2-DG (1 g/kg, twice a day), DHEA (100 mg/kg, twice a day), or Eto (35 mg/kg, twice a day). Four days later, splenocytes were subjected to surface $CD4^+$, $CD8^+$, and H-$2K^b$ staining, as well as intracellular flow cytometric staining for IFN-γ. (**A**) T cell proliferation and activation was determined as CFSE dilution and IFN-γ secretion. (**B** and **C**) Absolute numbers of H-$2K^{b+}$ donor T cells (**B**) and IFN-γ secreting donor T cells (**C**) in recipient spleens. (**D**) Profile of donor T cell proliferation reflected by CFSE dilution. (**E**) Summary of donor T cell proliferation reflected by %CFSE diluted cells. The data are representative of two independent experiments with at least 4 mice per group in each experiment. Data show mean ± SEM. $^*P < 0.05$; $^{**}P < 0.01$; $^{***}P < 0.001$, two-tailed Student *t* test (**B**, **D**, and **E**).

mTORC1 regulates T cell pathogenicity, likely through controlling glycolytic activity of allogeneic T cells after BMT, and that glycolysis rather than OXPHOS is the major metabolic pathway adopted by allogeneic T cells during the induction of GVHD.

mTOR/mTORC1 deficiency decreases donor T cell migration to GVHD target organs after BMT. To define the mechanisms by which mTOR/mTORC1 regulates GVHD, we first attempted to determine the migration pattern of donor T cells toward target organs, which is considered a crucial process required for GVHD induction. We observed remarkably fewer *Mtor* or *Raptor* KO $CD4^+$ or $CD8^+$ T cells than their WT counterparts in recipient livers (Figure 6A). However, there was a greater number of *Mtor*, *Raptor*, or *Rictor* KO $CD4^+$ or $CD8^+$ T cells than their respective WT counterparts in recipient spleens (Figure 6B). In contrast, no significant difference was seen in the numbers of $CD4^+$ or $CD8^+$ T cells in the livers of the recipients transplanted with *Rictor* WT or KO cells. We surmised that mTOR or RAPTOR might contribute to the migration of donor T cells into the livers and thus examined the molecules that control T cell migration. Chemokine receptors CXCR3 and CCR6 are known to support Th1 cell migration to the liver, gut, and skin and Th17 cell migration to the lung and skin, respectively (30, 31). Correlating with less pathologic injury (Figure 5G), the expression of CXCR3 (Figure 6B and Supplemental Figure 6A) and CCR6 (Supplemental Figure 6B) on donor $CD4^+$ and $CD8^+$ T cells in *Raptor* KO recipients were significantly decreased compared with the respective WT control. Similar trends were observed on donor $CD4^+$ T cells in *Mtor* or *Rictor* KO spleens. Likewise, *Mtor* or *Raptor* KO T cells also expressed markedly lower gut-homing receptor α4β7 versus WT control (data not shown). These results suggest that mTORC1, or mTOR, likely promotes T cell upregulation of chemokines and adhesion receptors, leading to T cell migration into GVHD target organs.

mTOR/mTORC1 deficiency decreases donor T cell proliferation and differentiation into Th1 phenotype but enhances generation of iTregs after BMT. To elucidate the effect of glycolysis impairment caused by ablation of mTOR/ mTORC1 on T cell alloresponses, we measured T cell activation and effector function during the development of GVHD in the absence of mTOR/mTORC1. Fourteen days after allogeneic BMT, $CD4^+$ *Mtor* or *Raptor* KO T cells produced remarkably lower levels of IFN-γ than their WT counterparts in recipient spleens or livers (Figure 6C). The absolute numbers of IFN-γ–producing $CD4^+$ or $CD8^+$ T cells were signifi-

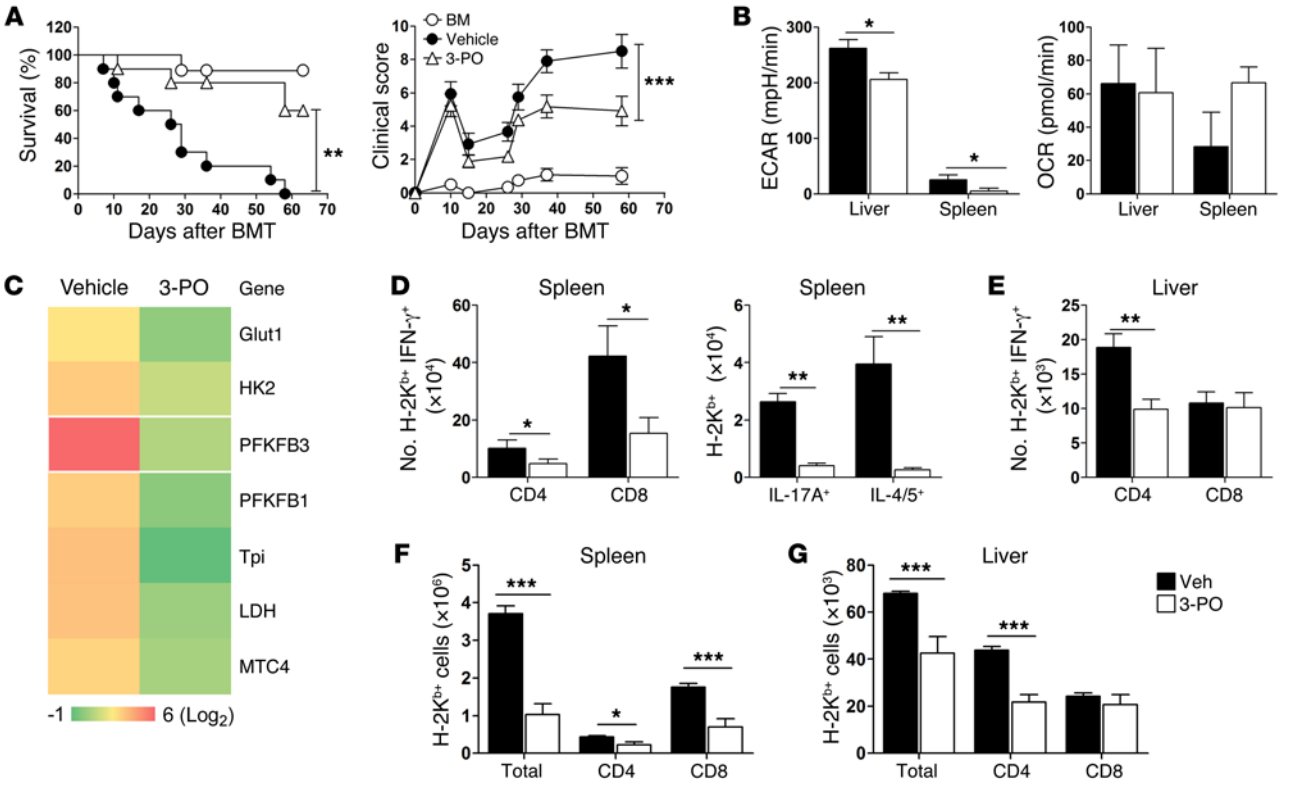

Figure 8. Inhibition of glycolysis by 3-PO significantly ameliorates GVHD after myeloablative allo-BMT. Lethally irradiated BALB/c mice (n = 10 per group) were transplanted with 5 × 10^6 TCD-BM alone or plus 1 × 10^6/mouse T cells from WT B6 donors. Recipients were daily injected i.p. with vehicle or 3-PO (35 mg/kg/day) beginning on the day of BMT for 4 weeks. (**A**) Recipient survival and clinical score from two independent experiments are shown. (**B**–**G**) In separate experiments, BALB/c recipients (n = 5–6 per group) were transplanted with 1 × 10^6 T cells from B6 donors and treated with vehicle or 3-PO (35 mg/kg/day) beginning on the day 0 and ending on day 7 when the experiment was terminated. (**B**) The ECAR and OCR values are shown on donor T cells from recipient spleens and livers were displayed. (**C**) The heat map represents the $\log_2$ value of the relative individual mRNA expression of glycolytic enzymes in splenic T cells. The list of genes input and expression profile are provided in Supplemental Table 6. (**D** and **E**) IFN-γ, IL-4/5, and IL-17 for H-2K^{b+} Ly5.1$^-$CD4$^+$ or H-2K^{b+}Ly5.1$^-$CD8$^+$ spleen or IFN-γ for liver T cells was shown. The absolute number of donor T cells in spleen (**F**) and liver (**G**) were displayed. Data show mean ± SEM and from a representative of two independent experiments; *P < 0.05; **P < 0.01; ***P < 0.001, log-rank test (**A**, left panel), Mann-Whitney U test (**A**, right panel), two-tailed Student t test (**B** and **D**–**G**).

cantly lower in the absence of mTOR or RAPTOR in recipient liver but not spleen (Figure 6, D and E). In the absence of RICTOR, a comparable or higher number of IFN-γ–producing CD4$^+$ or CD8$^+$ T cells in recipient livers or spleens was observed (Figure 6, C–E). The percentage and absolute numbers of IL-4/5–producing CD4$^+$ T cells in recipient livers and spleens were drastically increased in the absence of RICTOR, whereas a decrease was observed with *Raptor* KO T cells. Percentages of IL-17–secreting cells were low and similar among the seven types of donor T cells (data not shown). Because inhibition of glycolysis has been reported to promote iTreg generation (17, 32), we also analyzed donor-derived iTregs (CD4$^+$CD25$^+$Foxp3$^+$). As expected, low levels of iTregs were induced from WT donor CD4$^+$ T cells during GVHD development; however, donor-derived iTregs were significantly enhanced in the absence of mTOR or RAPTOR but not RICTOR (Figure 6, F and G). These data indicate that mTORC1 positively regulated Th1 differentiation and negatively regulated iTreg differentiation. Given that Th1 is pathogenic and iTreg is protective, with Th2 playing a negligible role in GVHD (33), enhanced iTreg generation might contribute to the little or no GVHD observed in the recipients of *Raptor* KO T cells.

The observed reduction of Th1 differentiation could be the result of reduced T cell activation and/or expansion. To test this possibility, we measured T cell activation and expansion early after cell transfer in allogeneic recipients. We observed that the absence of mTOR or RAPTOR significantly decreased donor T cell proliferation in allogeneic recipients, reflected by a dramatic reduction in CSFE-diluted cells (Supplemental Figure 5A). Furthermore, among proliferating cells, the percentages of IFN-γ–secreting CD8$^+$ T cells were significantly reduced in *Raptor* KO T cells. The percentages of IL-4/5– or IL-17–secreting T cells were not significantly altered in the various types of T cells (Supplemental Figure 5, B and C). However, the absolute number of IFN-γ–, IL-4/5–, and IL-17–secreting CD4$^+$ and CD8$^+$ T cells were dramatically decreased in *Raptor* KO T cells (Supplemental Figure 5, D and E). These data demonstrate that mTOR — or, more specifically, mTORC1 — is required for T cell expansion as well as optimal differentiation into Th1 phenotype.

Glycolysis is required for alloantigen-induced T cell activation and proliferation after BMT. Our genetic data has provided evidence that glycolysis is required for allogeneic T effector function in GVHD. However, mTORC1 not only promotes glycolysis, but

also lipid metabolism (17), which is attenuated in alloantigen-activated T cells as indicated by metabolomic analysis in the current study. Moreover, the upregulation of the PPP suggests this pathway may also contribute to activation, proliferation, and function of alloantigen-activated T cells after BMT. Therefore, it is essential to evaluate the potential impact of individual pathways on the metabolic reprogramming of T cells in response to alloantigens after BMT. We therefore applied a panel of potent chemical inhibitors (Supplemental Table 10) to target different metabolic pathways. We observed that inhibition of FAO by Etomoxir (Eto; a CPT1A inhibitor) or inhibition of PPP by dehydroepiandrosterone (DHEA; a glucose-6 phosphate dehydrogenase inhibitor) did not have a significant effect on donor T cell proliferation (Figure 7, A–E). In contrast, inhibition of glycolysis by 2-deoxy-D-glucose (2-DG) remarkably suppressed donor T cell proliferation reflected by reduced donor absolute cell counts and T cell division in recipient spleens (Figure 7, B–E). Furthermore, the percentage and absolute number of IFN-γ–secreting $CD4^+$ and $CD8^+$ T cells also significantly decreased in 2-DG–treated recipients (Figure 7, A and C). Thus, glycolysis is required for optimal proliferation and activation of T cells after allogeneic BMT.

Inhibition of glycolysis by targeting Pfkfb3 attenuates GVHD in vivo. The crucial role of glycolysis for alloantigen-activated T cell function suggests that glycolysis can be a therapeutic target for the control of GVHD. We initially tested 2-DG but found that short-term treatment was not effective enough to control GVHD and prolonged treatment had severe toxicity to recipients after allo-BMT. Seeking other pharmacological compounds with less toxicity and more selective glycolytic inhibition, we found that 3-(3-pyridinyl)-1-(4-pyridinyl)-2-propen-1-one (3-PO) — a specific inhibitor of PFKFB3 (34, 35), which is a regulatory and a rate-limiting factor in the glycolytic pathway (34, 36) — was well tolerated by the recipients of allo-BMT. We observed that the treatment with 3-PO significantly improved survival ($P < 0.01$) and reduced the GVHD clinical score ($P < 0.001$) as compared with vehicle controls (Figure 8A). These data demonstrate pharmacological inhibition of glycolysis effectively controls GVHD after allogeneic BMT.

To delineate the mechanisms via which 3-PO affects GVHD development, we first evaluated the effect of 3-PO on bioenergetic activity of T cells at an early stage after cell transfer in allogeneic recipients. We observed that 3-PO treatment profoundly decreased ECAR of T cells isolated from the spleens and livers of allogeneic recipients, whereas no significant effect on OCR was observed (Figure 8B). Consistently, the relative individual mRNA expression of glycolytic enzymes in splenic T cells was significantly diminished in recipients treated with 3-PO versus those treated with vehicle (Figure 8C). Noticeably, the mRNA level of *Pfkfb3*, the most significantly upregulated enzyme in the splenic T cells from vehicle mice, was drastically decreased by 3-PO treatment (Figure 8C). This suggests that inhibition of PFKFB3 resulted in diminished glycolytic activity of T cells, which may be a key mechanism ascribed for the protective action of 3-PO against GVHD. The percentages and absolute numbers of IFN-γ–secreting $CD4^+$ or $CD8^+$ T cells and IL-4/5– and IL-17–secreting $CD4^+$ T cells were significantly reduced in the spleen (Figure 8D and Supplemental Figure 7) or liver (Figure 8E) of the recipients treated with 3-PO. The absolute number of $CD4^+$ and $CD8^+$ T cells in the spleens and $CD4^+$ T cells in the liver of recipients treated with 3-PO were also remarkably decreased (Figure 8, F and G). Taken together, these data demonstrate that inhibition of glycolysis by 3-PO results in the reduction of donor T cell glycolytic activity, leading to alleviation of GVHD.

Discussion

In the current study, we observed a time-dependent metabolic change in T cells activated by alloantigens after BMT, and we provide solid evidence that metabolic reprogramming is associated with a global change in transcriptomes and the relative amount of metabolites in the context of GVHD. Similar to in vitro–activated T cells, in vivo–activated T cells increase glycolytic activity to meet their high-energetic demand for robust proliferation (9). In comparison with T cells in syngeneic recipients, alloantigen-activated T cells further increase glycolysis in allogeneic recipients, indicating that escalation of glucose metabolism may be attributed to GVHD development. The escalated glycolysis of donor T cells likely results from a strong and sustained stimulation by alloantigen-driving T cells to become pathogenic (2). Consistently, pharmacological inhibition of glycolysis, rather than other pathways, alters in vivo T cell activation and function, validating that glycolysis is critical for T cell proliferation and function in an allogeneic response after allo-BMT.

Metabolomic and genomic analyses in our current study provide evidence that alloantigen-activated T cells decrease FA and pyruvate oxidation in the TCA cycle, which may further impact the synthesis of macromolecules such as nucleotides and polyamines. Memory T cells and Tregs, in contrast to effector T cells, do not acquire appreciable amounts of extracellular-free FA, nor do they readily store exogenous long-chain FA in lipid droplets (37, 38). Hence, the accumulation of FAs in T cells after allogeneic BMT may indicate the effector phenotype of alloantigen-activated T cells in GVHD recipients. Like in vitro–activated T cells, alloantigens in in vivo–activated T cells couple glycolysis with PPP and glutaminolysis (9). Glutamine catabolism is not only used to replenish the intermediate metabolites of the TCA cycle, but also to coordinate with glucose catabolism by producing the anaplerotic substrate α-KG to support amino acid, nucleotide, and lipid biosynthesis. In this respect, Glick et al. recently showed that glutamine-dependent TCA cycle anaplerosis is increased in alloreactive T cells and that glutamine carbon contributes to ribose biosynthesis (39). While we failed to detect α-KG, likely due to technological sensitivity, the increased expression of mRNA coding for glutaminolysis-regulating enzymes GLUT1, OAT, and GOT and the metabolite Asp and Orn suggest an increased glutamine metabolism in allogeneic T cells after BMT (40). Consistently, the polyamine metabolites and ODC expression were increased in allogeneic T cells. Furthermore, pyrimidine catabolism was significantly decreased, implying an increase in the biosynthesis of macromolecules in allogeneic T cells. Despite the increased PPP activity in alloantigen-activated T cells, blockade of PPP pathway did not show a significant effect on proliferation and activation of $CD4^+$ T cells in vivo that was observed in in vitro–activated T cells (9), indicating that in vivo alloantigen-activated T cells may use pathways other than PPP to support macromolecule biosynthesis during proliferation and activation.

Gatza et al. showed that donor T cells, in response to alloantigens in the context of GVHD, greatly increase both glycolysis and OXPHOS and that the increase in OXPHOS was concluded to be due to an increase of FAO in the TCA cycle (12). However, the unirradiated B6 → B6D2F1 GVHD model in their study does not accurately represent clinical circumstances in which patients are typically preconditioned. To define the metabolic profile of proliferating BM cells, they analyzed the BM cells harvested from the recipients of syngeneic BM graft using BM cells from naive donors as the control, which does not represent the metabolic profile of the BM from the recipients of an allogeneic BM graft. Furthermore, they used the bioenergetics of the BM cells as a baseline to compare with activated T cells after allo-BMT, which may not be appropriate. Moreover, they compared the donor T cells retrieved from the allogeneic recipients to resting T cells instead of the donor T cells from syngeneic recipients. It is plausible that the metabolic profile of resting T cells is very different from the donor T cells retrieved even from syngeneic recipients after BMT, given homeostatic proliferation under an inflammatory environment as shown in the current study. In addition, they utilized GLUT1 expression as an important index to make a conclusion that FAs, rather than glucose, may be the principal substrates for ATP generation in alloreactive T cells (12). However, contrary to a previous report that GLUT1 is the major glucose transporter in hematopoietic cells (10), we observed that the mRNA level of *Glut3* is also higher in T cells from allogeneic recipients than from syngeneic recipients. Interestingly, the difference in the copy number of *Glut3* in allogeneic recipient T cells is more prominent than that of *Glut1*, suggesting a distinct glucose transporter expression in alloantigen-activated T cells. The extremely low amounts of the glycolytic substrate pyruvate observed in their study could be due to the fact that glucose-generated pyruvate in alloactivated T cells was converted to lactate instead of metabolized in the TCA cycle because they also observed the increased lactate generation in alloreactive T cells. Along the same lines, a recent publication from Byersdorfer et al. reported that FAO through TCA cycle is the major energetic resource for alloreactive T cells in which naive T cells were again utilized as the control (11). In contrast, we observed that inhibition of FAO did not impair proliferation and function of alloreactive T cells, demonstrating that FAO may not play an important role in T cell proliferation and function during an allogeneic response in vivo. Alloreactive T cells likely use FA as a material resource available for cell division rather than as a fuel resource. In agreement with this assumption, pathogenic T cells were recently reported to depend on de novo FA synthesis and an underlying glycolytic-lipogenic metabolic pathway for their development (37). Increases in FAO did not occur after allogeneic T cell activation (11), proving that alloantigen-activated T cells still use glycolysis as a major pathway for gaining energy, at least in early stages of GVHD. Consistently, in the current study, we observed that T cells retrieved from allogeneic recipients decreased FA uptake after BMT, providing solid evidence that FA is not a major energy resource for allogeneic T cells. In support of this, the intracellular protein expression of CPT1A was unchanged in alloantigen-activated T cells. Moreover, mRNA levels of coactivator *Pgc1a*, another key transcriptional regulator of FAO that enhances OXPHOS and represses glycolysis through the action of multiple other coactivators and transcription factors, was comparable in T cells from allogeneic and syngeneic recipients. Collectively, these data suggest that the difference in FAO and OXPHOS likely does not contribute to the pathogenicity of donor T cells. Because FAO is involved in fueling the energy for memory T cells (41), and given that there was no surface marker phenotype for alloreactive T cells shown, it is likely that the study from Ferrera's group was mainly targeting the memory phenotype (11). On the contrary, glycolytic activity was always significantly increased in T cells under alloantigen activation compared with those under homeostatic proliferation, implying that inhibition of glycolysis may preferentially affect pathogenic T cells for the control of GVHD. Along these lines, an elegant study by Rathmell's group shows that $CD4^+$ T cells deficient for GLUT1, which is required for glucose uptake and glycolysis, had a drastically reduced capacity to mount allogeneic responses in vivo (10).

The mTOR signaling pathway plays a crucial role in promoting glucose metabolism (42–44). In line with previous reports, the current study shows that genetic depletion of *Mtor* or mTORC1 not only impairs the glycolytic activity but also diminishes the ability of allogeneic T cells to induce GVHD. We also show that mTORC2 was not responsible for GVHD induction, indicating distinct roles of mTORC1 and mTORC2 in T cell pathogenicity. As glycolysis is required for normalizing function of alloantigen-activated T cells (5, 10), impeding glycolysis due to the absence of mTORC1 likely contributes to downregulation of donor T cell activation, proliferation, differentiation, and function, thereby disabling alloreactive T cells to induce GVHD. In support of the genetic analysis, the mTORC1 inhibitor rapamycin also selectively decreased the glycolytic activity of donor T cells in allogeneic recipients.

Aerobic glycolysis is closely linked with cell growth as it assists in increasing mass for cell proliferation (45). Therefore, ablation of mTORC1 suppresses T cell activation and proliferation, possibly as a consequence of inadequate nutrients to support biosynthesis induced by mTORC1. Maintenance of glycolysis is imperative for T cells to secrete IFN-γ (46, 47), and glycolytic flux has been implicated in IFN-γ translation (24). We observed mTORC1-deficient T cells had a reduction in IFN-γ production. IFN-γ–secreting T cells were drastically decreased in peripheral lymphoid and GVHD target organs in the recipients of mTORC1-deficient donor T cells. Consistently, the serum levels of IFN-γ were also significantly reduced in those recipients. Glycolysis is required for CD4 T cell differentiation into Th1 and Th17 (5). Inhibition of glycolysis promotes iTreg generation (32). Moreover, lactic acid, the end product of glycolysis, also skews $CD4^+$ T cells toward Th17 (48). Indeed, we found both reduced cell numbers and decreased inflammatory cytokine production by mTORC1-deficient Th1 and Th17 cells. In addition, a significant increase in the absolute number of RAPTOR-deficient iTregs was observed in peripheral lymph nodes of recipients after allo-BMT. While Th1 and Th17 pathogenicity is crucial for the development of GVHD (33), with Tregs being protective (49), alteration of T cell differentiation due to lack of RAPTOR likely contributes to the impaired ability of T cells to induce GVHD. Since mTORC1 is required for iTreg-suppressive function (17), the role of iTregs in GVHD prevention is expected to be minor. Donor T cell infiltration into target organs is a prerequisite for

GVHD development, and chemokine receptor expression is vital to T cell migration. Glycolytic activity was shown to be required to maintain cell migratory properties of effector T lymphocytes (50). Indeed, we found fewer *Raptor* KO T cells in recipient livers, possibly due to reduced liver-homing receptor CXCR3 and CCR6 expression, which were correlated with less tissue injury compared with WT T cells. Additionally, less GVHD-related colon pathology was observed in the recipients of *Raptor* KO T cells, which likely resulted from lower expression of α4β7, an integrin required for intestine-specific trafficking (51). These observations are consistent with the report that mTORC1 is required to sustain glycolysis, which controls the expression of essential chemokine (e.g., CXCR3), and adhesion receptors that regulate T cell trafficking (52). Recently, lactate was reported to be responsible for pathogenic T cell entrapment in inflammatory sites, where they perpetuate inflammation (48). Our data provide evidence that glycolysis also regulates chemokine receptors or adhesion molecules, although it is unclear whether this is a direct or secondary effect due to impaired T cell activation overall.

While mTOR inhibitors are considered strong immunosuppressive drugs, the clinical outcomes from GVHD treatment are quite controversial (28, 53, 54). Therefore, it is unclear whether mTOR is a valid target for the prevention of acute GVHD. The current study provides strong evidence that mTORC1, not mTORC2, is a valid therapeutic target to control GVHD through regulating glycolysis of T cells. We reason that the major obstacle for effective treatment regarding blocking mTOR signaling may relate to the high toxicity and low selectivity of clinical mTOR inhibitors. Therefore, novel inhibitors that are more effective and specific for mTORC1 are highly warranted to overcome the challenge.

A study showing that metabolic inhibition of glycolysis and/or glutamine metabolism to regulate alloreactive T cell responses results in the prevention of allograft rejection has been recently reported (7). Along the same lines, we show here that 3-PO, a glycolysis inhibitor at PFKFB3 (55), effectively attenuated GVHD in a preclinical BMT model. A similar effect on GVHD was also obtained by using PFK15, another PFKFB3 inhibitor (data not shown). T cell activation is associated with a rapid increase in intracellular fructose-2, 6-bisphosphate (F2,6BP), an allosteric activator of the glycolytic enzyme 6-phosphofructo-1-kinase (PFK-1) (36), which was drastically upregulated in allogeneic T cells in current study. The steady state concentration of F2,6BP in T cells is dependent on the expression of the bifunctional 6-phosphofructo-2-kinase/fructose-2,6-bisphosphatases (PFKFB1-4) and the fructose-2,6-bisphosphatase, TIGAR (56). Of the PFKFB family, PFKFB3 has the highest kinase/bisphosphatase ratio (57) and is the most markedly upregulated in activated T cells, enabling the metabolic switch from OXPHOS to aerobic glycolysis. PFKFB3 has been demonstrated to be required for T cell proliferation and function (3, 58). We observed that treatment with 3-PO in vivo was associated with significantly diminished *Pfkfb3* gene expression and glycolytic activity of donor T cells in recipients after BMT, suggesting a critical role of PFKFB3 in maintaining glycolysis for allogeneic T cell survival, activation, and function. In addition to its effect on T cells, 3-PO may also reduce GVHD by affecting antigen-presenting cells and endothelial cells (35). Among others, we speculate that PFKFB3 inhibitors may have unidentified pleiotropic effects on the immune system that may contribute to its ability to prevent GVHD.

In conclusion, the current study shows a distinct metabolic profile of alloantigen-activated T cells in vivo, which are distinguished from that of in vitro–activated T cells and of pathogenic T cells in other autoimmune diseases. Furthermore, glycolysis is required for alloantigen-activated T cells to induce GVHD. Inhibition of glycolysis through specifically targeting mTORC1 or PFKFB3 ameliorates GVHD mortality and morbidity. Thus, the current work clearly identifies glycolysis as the predominant metabolic pathway in donor T cells after allogeneic HCT and further validates glycolysis as a potential therapeutic target for the control of GVHD. Future studies should address the effect of glycolysis inhibition on graft versus leukemia (GVL) activity.

Methods

Mice. C57BL/6 (H-2^b, CD45.2), B6.Ly5.1 (H-2^b, CD45.1), B6D2F1 (H-$2^{b/d}$, CD45.2), and BALB/c (H-2^d) mice were purchased from NIH. *Mtor*, *Raptor*/*Rictor* KO, and their WT controls were provided by H. Chi's lab (14, 27).

Cell preparation. T cells were purified from pooled spleen and lymph node by negative selection to remove non–T cells including B cells, natural killer (NK) cells, DCs, macrophages, granulocytes, and erythroid cells as described before (59). Briefly, non–T cells were indirectly magnetically labeled by using a cocktail of biotin-conjugated Abs against CD45R (B220) (eBioscience, clone RA3-B2), CD49b (DX5) (eBioscience, clone DX5); CD11b (Mac-1) (eBioscience, clone M1/70), and Ter-119 (eBioscience, clone Ter-119), as well as anti-biotin MicroBeads (Miltenyi Biotec). Isolation of T cells was achieved by depletion of the magnetically labeled cells. T cell–depleted BM (TCD-BM) was prepared from donor tibia and femurs with anti-Thy1.2 Abs (Bio X cell) and complement incubation (59).

GVHD models. Recipient mice were lethally irradiated at 700 cGy for BALB/c and 1,200 cGy (2 split doses, 3-hour interval) for B6 or B6D2F1 mice using an X-RAD 320 irradiator (Precision X-Ray). Syngeneic (B6) or allogeneic (BALB/c or B6D2F1) irradiated mice were transplanted with 5.0×10^6/mouse TCD-BM from B6 or B6.Ly5.1 donors with or without T cells ($0.5–1.0 \times 10^6$/mouse). Recipient survival was followed throughout the experiment. The development of GVHD was monitored twice per week for weight loss and once per week for clinical signs of posture, skin damage, hair loss, ruffled fur, diarrhea, and decreased activity. In some experiments, donor T cells were labeled with 2.5 μM CFSE (Invitrogen) and transplanted into irradiated recipients.

Histologic analysis. Representative samples of liver, small intestine, large intestine, lung, and skin were obtained from transplanted recipients 7 or 14 days after transplant; fixed in 10% neutral-buffered formalin; and washed with 70% ethanol. Samples were then embedded in paraffin, cut into 5-μm thick sections, and stained with H&E. A semiquantitative scoring system was used to account for histologic changes consistent with GVHD in the colon, liver, and lung as previously described (60). Data were presented as individual GVHD target organ. All slides for GVHD analysis were coded and read in a blinded fashion (59).

Lymphocyte isolation from recipient liver. Livers were homogenized and passed through a 70-μm cell strainer. Pellets were resuspended in PBS, overlaid on Ficoll (Sigma-Aldrich), and centrifuged at 500 *g* for 20 minutes. Lymphocytes were recovered from the interface (60).

Metabolic assays. The metabolic profile of single-cell suspensions was determined using a Seahorse XF96 Analyzer (Seahorse Bioscience). Briefly, T cells (0.5–1.0 × 10^6/well) were attached to tissue culture plates for 30 minutes using Cell-Tak (BD Biosciences, catalog 354240) (61). OCR were analyzed in response to 1.0 μM oligomycin, 1.0 μM fluoro-carbonyl cyanide phenylhydrazone (FCCP), and 2 μM rotenone (Seahorse Bioscience) plus 100 nM antimycin A (Sigma-Aldrich). ECAR were measured under basal conditions and following injection of three pharmacologic compounds: glucose (5.5 mM), oligomycin (1.0 μM), and 2-DG (100 mM) (62).

Metabolic profiling. Unbiased metabolomic profiling was performed by Metabolon Inc. Lethally irradiated B6 (syngeneic) or BALB/c (allogeneic) recipients were transplanted with T cells and BM cells freshly isolated from B6 donors. Four, 7, and 14 days after BMT, T cells were isolated from recipient spleens for metabolite profiling. All the samples were extracted and analyzed through UPHPLC/MS/MS and GC/MS. Data were then grouped by unsupervised clustering using MetaboAnalyst software. Samples were loaded in an equivalent manner across the platform and normalized to total protein, as determined by Bradford analysis prior to statistical analysis.

RNA isolation, reverse transcription, and quantitative PCR. Total RNA was isolated from T cells using Trizol (Invitrogen). cDNA was generated from 1 μg total RNA using iScript cDNA Synthesis Kit (Bio-Rad). SYBR Green incorporation of quantitative PCR (qPCR) was performed using a SYBR Green mix in the CFX96 Detection System (Bio-Rad). Samples for each experimental condition were run in triplicate and were normalized to β-2 microglobulin. Primer sequences were obtained from PrimerBank (63). Primer sequences are listed in Supplemental Table 9.

Abs, flow cytometry, and cytometric bead assay. The following Abs were used for cell-surface staining: anti–CD4-V450, -APC, and -PEcy7 (BD Biosciences, clone RM4-5); anti–CD8-PEcy5, -APCcy7, and -AF700 (BD Biosciences, clone 53-6.7); anti–CD45.1-FITC, -BV711, and -APC (BD Biosciences, clone A20); anti–B220-FITC and -PE (eBioscience, clone RA3-6B2); anti–H-$2K^b$-FITC, -APC, and –PerCP-eFluor 710 (eBioscience, clone AF6-88.5.5.3), anti–CXCR3-biotin (eBioscience, clone CXCR3-173); and anti–CCR6-AF647 (BioLegend, clone 29-2L17). Detection of biotinylated Abs was performed using APCcy7 (BD Biosciences, catalog 554063) or PEcy7 (BD Biosciences, catalog 557598) conjugated to streptavidin. GLUT1 expression was stained using rabbit anti–mouse-GLUT1 (Abcam, clone SPM498) fixed with 2% paraformaldehyde at room temperature for 20 minutes followed by incubation with AF488-conjugated goat anti-Mouse (H+L) IgG (Invitrogen, catalog a-11001) (64). To measure intracellular cytokines, cells were left unstimulated or stimulated for 4–5 hours at 37°C with phorbol myristate acetate (100 ng/ml, Sigma-Aldrich) and ionomycin (500 ng/ml; Calbiochem, EMD) in the presence of GolgiPlug (BD Biosciences, catalog 555029) or GolgiStop (BD Biosciences, catalog 554724), permeabilized using Cytofix/Cytoperm Plus (BD Biosciences, catalog 554722), and then stained with the appropriate Abs including (65) anti–IFNγ-APC or –PerCP 5.5 (eBioscience, clone XMG1.2); anti–IL-17–PE/Cy7 (BioLegend, clone TC11-18H10.1); anti–IL-4–PE (BD Biosciences, clone 11B11); anti–IL-5–PE (BD Biosciences, clone TRFK5); anti–FOXP3-PE or -APC (eBioscience, clone FJK-16s), and appropriate isotype controls. Live/dead yellow dead cell staining kit (catalog L-34968) and CFSE (catalog C1157) were purchased from Invitrogen. For glucose uptake assay, T cells were incubated with 100 μM 2-NBDG (Cayman Chemical, item no. 11046) for 10 minutes before measuring fluorescence by flow cytometry. To measure FA uptake, cells were washed twice with 37°C PBS and resuspended in 6 μM $BoDipy_{C1\text{-}C12}$ (Invitrogen, catalog D-3823) in 20 μM FA containing BSA-free PBS for 5 minutes. BoDipy uptake was quenched by adding 4× volumes of ice-cold PBS containing 2% FBS. Cells were washes twice prior to analysis. To measure the intracellular level of pS6 and CPT1A, cells were permeabilized using Cytofix/Cytoperm Plus, then stained with anti–pS6-AF467 (Cell Signaling Technology, clone D57.2.2E) and anti–CPT1A-AF488 (Abcam, catalog ab171449, clone 8F6AE9) or appropriate isotypes. Analysis was performed on a LRS Fortessa or FACS Verse (BD Biosciences). Data were analyzed using FlowJo (Tree Star Inc.). Blood was collected from recipients 14 days after BMT, and serum cytokine quantification was conducted using a cytometric bead assay kit (BD Biosciences, catalog 560485) (66, 67).

Statistics. Data were analyzed using Prism GraphPad (version 5 or 6). Briefly, comparisons between two groups were calculated using two-tailed Student *t* test. Clinical scores and body weight loss were compared using a nonparametric Mann-Whitney *U* test. The log-rank (Mantel-Cox) test was utilized to analyze survival data. Statistical analysis of metabolism data was performed by Welch's *t* tests, Wilcoxon's rank sum tests, and/or one-way ANOVA followed by the Dunnett's test. A *P* value less 0.05 was considered significant.

Study approval. All mice were housed in a pathogen-free facility at the American Association for Laboratory Animal Care–accredited Animal Resource Center at Medical University of South Carolina. All animal studies were carried out under protocols approved by the Institutional Animal Care and Use Committee at Medical University of South Carolina.

Author contributions

HDN, HC, SM, and XZY participated in designing research studies. HDN, SC, KMKH, YW, DB, JH, JF, AD, S Schutt, and S Shrestha participated in conducting experiments and acquiring data. HDN, SC, KMKH, and XZY participated in analyzing data. HDN and XZY participated in interpreting data. HDN, DB, HC, SM, and XZY participated in writing the manuscript. HDN, DB, S Shrestha, HC, SM, and XZY participated in editing the manuscript. HDN, DB, S Shrestha, HW, HC, SM, and XZY participated in revising the manuscript. CL performed pathological analysis. HC provided genetic KO mice.

Acknowledgments

We are grateful to Ruoning Wang for his review and comments to improve the quality of this manuscript. We acknowledge Gyda Beeson and Craig Beeson and their lab at Medical University of South Carolina for their full support of bioenergetic analysis. We thank the members of the FACS and Metabolomic Core Facility and Supinya Iamsawat at Medical University of South Carolina. This work is partially supported by grants R01 AI118305, R01 CA169116, CA118116, CA169116, and R21 CA192202 (to X.Z. Yu).

Address correspondence to: Xue-Zhong Yu, Department of Microbiology and Immunology, MSC 955, Medical University of South Carolina, 86 Jonathan Lucas Street, Charleston, South Carolina 29425-5090, USA. Phone: 843.792.4756; E-mail: yux@musc.edu.

1. Ferrara JL, Levine JE, Reddy P, Holler E. Graft-versus-host disease. *Lancet*. 2009;373(9674):1550–1561.
2. Wahl DR, Petersen B, Warner R, Richardson BC, Glick GD, Opipari AW. Characterization of the metabolic phenotype of chronically activated lymphocytes. *Lupus*. 2010;19(13):1492–1501.
3. Yang Z, Fujii H, Mohan SV, Goronzy JJ, Weyand CM. Phosphofructokinase deficiency impairs ATP generation, autophagy, and redox balance in rheumatoid arthritis T cells. *J Exp Med*. 2013;210(10):2119–2134.
4. Biniecka M, et al. Hypoxia induces mitochondrial mutagenesis and dysfunction in inflammatory arthritis. *Arthritis Rheum*. 2011;63(8):2172–2182.
5. Gerriets VA, et al. Metabolic programming PDHK1 control $CD4^+$ T cell subsets inflammation. *J Clin Invest*. 2015;125(1):194–207.
6. Gerriets VA, Rathmell JC. Metabolic pathways in T cell fate and function. *Trends Immunol*. 2012;33(4):168–173.
7. Lee CF, et al. Preventing allograft rejection by targeting immune metabolism. *Cell Rep*. 2015;13(4):760–770.
8. Jones RG, Thompson CB. Revving the engine: signal transduction fuels T cell activation. *Immunity*. 2007;27(2):173–178.
9. Wang R, et al. The transcription factor Myc controls metabolic reprogramming upon T lymphocyte activation. *Immunity*. 2011;35(6):871–882.
10. Macintyre AN, et al. The glucose transporter Glut1 is selectively essential for CD4 T cell activation and effector function. *Cell Metab*. 2014;20(1):61–72.
11. Byersdorfer CA, et al. Effector T cells require fatty acid metabolism during murine graft-versus-host disease. *Blood*. 2013;122(18):3230–3237.
12. Gatza E, et al. Manipulating the bioenergetics of alloreactive T cells causes their selective apoptosis and arrests graft-versus-host disease. *Sci Transl Med*. 2011;3(67):67ra8.
13. Pearce EL, Poffenberger MC, Chang CH, Jones RG. Fueling immunity: insights into metabolism and lymphocyte function. *Science*. 2013;342(6155):1242454.
14. Chi H. Regulation and function of mTOR signalling in T cell fate decisions. *Nat Rev Immunol*. 2012;12(5):325–338.
15. Delgoffe GM, et al. The mTOR kinase differentially regulates effector and regulatory T cell lineage commitment. *Immunity*. 2009;30(6):832–844.
16. Yang K, et al. T cell exit from quiescence and differentiation into Th2 cells depend on Raptor-mTORC1-mediated metabolic reprogramming. *Immunity*. 2013;39(6):1043–1056.
17. Zeng H, Yang K, Cloer C, Neale G, Vogel P, Chi H. mTORC1 couples immune signals and metabolic programming to establish T(reg)-cell function. *Nature*. 2013;499(7459):485–490.
18. Laplante M, Sabatini DM. mTOR signaling at a glance. *J Cell Sci*. 2009;122(pt 20):3589–3594.
19. Delgoffe GM, et al. The kinase mTOR regulates the differentiation of helper T cells through the selective activation of signaling by mTORC1 and mTORC2. *Nat Immunol*. 2011;12(4):295–303.
20. Foster DA, Toschi A. Targeting mTOR with rapamycin: one dose does not fit all. *Cell Cycle*. 2009;8(7):1026–1029.
21. Marti HP, Frey FJ. Nephrotoxicity of rapamycin: an emerging problem in clinical medicine. *Nephrol Dial Transplant*. 2005;20(1):13–15.
22. Fox CJ, Hammerman PS, Thompson CB. The Pim kinases control rapamycin-resistant T cell survival and activation. *J Exp Med*. 2005;201(2):259–266.
23. Frauwirth KA, et al. The CD28 signaling pathway regulates glucose metabolism. *Immunity*. 2002;16(6):769–777.
24. Chang CH, et al. Posttranscriptional control of T cell effector function by aerobic glycolysis. *Cell*. 2013;153(6):1239–1251.
25. Gatenby RA, Gawlinski ET. The glycolytic phenotype in carcinogenesis and tumor invasion: insights through mathematical models. *Cancer Res*. 2003;63(14):3847–3854.
26. Filosa S, et al. Failure to increase glucose consumption through the pentose-phosphate pathway results in the death of glucose-6-phosphate dehydrogenase gene-deleted mouse embryonic stem cells subjected to oxidative stress. *Biochem J*. 2003;370(pt 3):935–943.
27. Waickman AT, Powell JD. mTOR, metabolism, and the regulation of T-cell differentiation and function. *Immunol Rev*. 2012;249(1):43–58.
28. Blazar BR, Taylor PA, Panoskaltsis-Mortari A, Vallera DA. Rapamycin inhibits the generation of graft-versus-host disease- and graft-versus-leukemia-causing T cells by interfering with the production of Th1 or Th1 cytotoxic cytokines. *J Immunol*. 1998;160(11):5355–5365.
29. Lee K, et al. Mammalian target of rapamycin protein complex 2 regulates differentiation of Th1 and Th2 cell subsets via distinct signaling pathways. *Immunity*. 2010;32(6):743–753.
30. Crome SQ, Wang AY, Kang CY, Levings MK. The role of retinoic acid-related orphan receptor variant 2 and IL-17 in the development and function of human $CD4^+$ T cells. *Eur J Immunol*. 2009;39(6):1480–1493.
31. Sackstein R. A revision of Billingham's tenets: the central role of lymphocyte migration in acute graft-versus-host disease. *Biol Blood Marrow Transplant*. 2006;12(1 suppl 1):2–8.
32. Shi LZ, et al. HIF1α-dependent glycolytic pathway orchestrates a metabolic checkpoint for the differentiation of TH17 and Treg cells. *J Exp Med*. 2011;208(7):1367–1376.
33. van der Waart AB, van der Velden WJ, Blijlevens NM, Dolstra H. Targeting the IL17 pathway for the prevention of graft-versus-host disease. *Biol Blood Marrow Transplant*. 2014;20(6):752–759.
34. Clem BF, et al. Targeting 6-phosphofructo-2-kinase (PFKFB3) as a therapeutic strategy against cancer. *Mol Cancer Ther*. 2013;12(8):1461–1470.
35. Schoors S, et al. Partial and transient reduction of glycolysis by PFKFB3 blockade reduces pathological angiogenesis. *Cell Metab*. 2014;19(1):37–48.
36. Van Schaftingen E, Hue L, Hers HG. Fructose 2,6-bisphosphate, the probably structure of the glucose- and glucagon-sensitive stimulator of phosphofructokinase. *Biochem J*. 1980;192(3):897–901.
37. Berod L, et al. De novo fatty acid synthesis controls the fate between regulatory T T helper 17 cells. *Nat Med*. 2014;20(11):1327–1333.
38. O'Sullivan D, et al. Memory CD8(+) T cells use cell-intrinsic lipolysis to support the metabolic programming necessary for development. *Immunity*. 2014;41(1):75–88.
39. Glick GD, et al. Anaplerotic metabolism of alloreactive T cells provides a metabolic approach to treat graft-versus-host disease. *J Pharmacol Exp Ther*. 2014;351(2):298–307.
40. Carey BW, Finley LW, Cross JR, Allis CD, Thompson CB. Intracellular alpha-ketoglutarate maintains the pluripotency of embryonic stem cells. *Nature*. 2015;518(7539):413–416.
41. van der Windt GJ, et al. CD8 memory T cells have a bioenergetic advantage that underlies their rapid recall ability. *Proc Natl Acad Sci U S A*. 2013;110(35):14336–14341.
42. Duvel K, et al. Activation of a metabolic gene regulatory network downstream of mTOR complex 1. *Mol Cell*. 2010;39(2):171–183.
43. Powell JD, Pollizzi KN, Heikamp EB, Horton MR. Regulation of immune responses by mTOR. *Annu Rev Immunol*. 2012;30:39–68.
44. Zheng Y, Delgoffe GM, Meyer CF, Chan W, Powell JD. Anergic T cells are metabolically anergic. *J Immunol*. 2009;183(10):6095–6101.
45. Vander Heiden MG, Cantley LC, Thompson CB. Understanding the Warburg effect: the metabolic requirements of cell proliferation. *Science*. 2009;324(5930):1029–1033.
46. Jacobs SR, Michalek RD, Rathmell JC. IL-7 is essential for homeostatic control of T cell metabolism in vivo. *J Immunol*. 2010;184(7):3461–3469.
47. Cham CM, Gajewski TF. Glucose availability regulates IFN-gamma production and p70S6 kinase activation in $CD8^+$ effector T cells. *J Immunol*. 2005;174(8):4670–4677.
48. Haas R, et al. Lactate regulates metabolic and pro-inflammatory circuits in control of T cell migration and effector functions. *PLoS Biol*. 2015;13(7):e1002202.
49. Komanduri KV, Champlin RE. Can Treg therapy prevent GVHD? *Blood*. 2011;117(3):751–752.
50. Sukumar M, et al. Inhibiting glycolytic metabolism enhances $CD8^+$ T cell memory and antitumor function. *J Clin Invest*. 2013;123(10):4479–4488.
51. Lu SX, et al. Absence of P-selectin in recipients of allogeneic bone marrow transplantation ameliorates experimental graft-versus-host disease. *J Immunol*. 2010;185(3):1912–1919.
52. Finlay DK, et al. PDK1 regulation of mTOR and hypoxia-inducible factor 1 integrate metabolism and migration of $CD8^+$ T cells. *J Exp Med*. 2012;209(13):2441–2453.
53. Pulsipher MA, et al. The addition of sirolimus to tacrolimus/methotrexate GVHD prophylaxis in children with ALL: a phase 3 Children's Oncology Group/Pediatric Blood and Marrow Transplant Consortium trial. *Blood*. 2014;123(13):2017–2025.
54. Pulsipher MA, et al. A phase I/II study of the safety and efficacy of the addition of sirolimus to tacrolimus/methotrexate graft versus host disease prophylaxis after allogeneic haematopoietic cell transplantation in paediatric acute lymphoblastic leukaemia (ALL). *Br J Haematol*. 2009;147(5):691–699.
55. Yalcin A, et al. Nuclear targeting of 6-phosphofructo-2-kinase (PFKFB3) increases proliferation via cyclin-dependent kinases. *J Biol Chem*. 2009;284(36):24223–24232.
56. Rider MH, Bertrand L, Vertommen D, Michels

PA, Rousseau GG, Hue L. 6-phosphofructo-2-kinase/fructose-2,6-bisphosphatase: head-to-head with a bifunctional enzyme that controls glycolysis. *Biochem J*. 2004;381(pt 3):561–579.
57. Yalcin A, Telang S, Clem B, Chesney J. Regulation of glucose metabolism by 6-phosphofructo-2-kinase/fructose-2,6-bisphosphatases in cancer. *Exp Mol Pathol*. 2009;86(3):174–179.
58. Telang S, et al. Small molecule inhibition of 6-phosphofructo-2-kinase suppresses t cell activation. *J Transl Med*. 2012;10:95.
59. Haarberg KM, et al. Pharmacologic inhibition of PKCα and PKCtheta prevents GVHD while preserving GVL activity in mice. *Blood*. 2013;122(14):2500–2511.
60. Liang Y, et al. β2 Integrins separate graft-versus-host disease and graft-versus-leukemia effects. *Blood*. 2008;111(2):954–962.
61. Capasso M, et al. HVCN1 modulates BCR signal strength via regulation of BCR-dependent generation of reactive oxygen species. *Nat Immunol*. 2010;11(3):265–272.
62. Everts B, et al. Commitment to glycolysis sustains survival of NO-producing inflammatory dendritic cells. *Blood*. 2012;120(7):1422–1431.
63. Spandidos A, Wang X, Wang H, Seed B. PrimerBank: a resource of human and mouse PCR primer pairs for gene expression detection and quantification. *Nucleic Acids Res*. 2010;38(Database issue):D792–D799.
64. Chan O, Burke JD, Gao DF, Fish EN. The chemo kine CCL5 regulates glucose uptake and AMP kinase signaling in activated T cells to facilitate chemotaxis. *J Biol Chem*. 2012;287(35):29406–29416.
65. Iclozan C, et al. T helper17 cells are sufficient but not necessary to induce acute graft-versus-host disease. *Biol Blood Marrow Transplant*. 2010;16(2):170–178.
66. Yu XZ, Liang Y, Nurieva RI, Guo F, Anasetti C, Dong C. Opposing effects of ICOS on graft-versus-host disease mediated by CD4 and CD8 T cells. *J Immunol*. 2006;176(12):7394–7401.
67. Gruber T, et al. PKC theta cooperates with PKC alpha in alloimmune responses of T cells in vivo. *Mol Immunol*. 2009;46(10):2071–2079.